

## Review

# Intracellular $\text{Na}^+$ regulation in cardiac myocytes

 Donald M. Bers<sup>a,\*</sup>, William H. Barry<sup>b</sup>, Sanda Despa<sup>a</sup>
<sup>a</sup>Department of Physiology, Loyola University Chicago, Stritch School of Medicine, 2160 South First Avenue, Maywood, IL 60153, USA

<sup>b</sup>Division of Cardiology, University of Utah, Health Science Center, Salt Lake City, UT 84132, USA

Received 8 July 2002; accepted 2 September 2002

## Abstract

Intracellular  $[\text{Na}^+]$  ( $[\text{Na}^+]_i$ ) is regulated in cardiac myocytes by a balance of  $\text{Na}^+$  influx and efflux mechanisms. In the normal cell there is a large steady state electrochemical gradient favoring  $\text{Na}^+$  influx. This potential energy is used by numerous transport mechanisms, including  $\text{Na}^+$  channels and transporters which couple  $\text{Na}^+$  influx to either co- or counter-transport of other ions and solutes. Six sarcolemmal  $\text{Na}^+$  influx pathways are discussed in relatively quantitative terms:  $\text{Na}^+$  channels,  $\text{Na}^+/\text{Ca}^{2+}$  exchange,  $\text{Na}^+/\text{H}^+$  exchange,  $\text{Na}^+/\text{Mg}^{2+}$  exchange,  $\text{Na}^+/\text{HCO}_3^-$  cotransport and  $\text{Na}^+/\text{K}^+/\text{2Cl}^-$  cotransport. Under normal conditions  $\text{Na}^+/\text{Ca}^{2+}$  exchange and  $\text{Na}^+$  channels are the dominant  $\text{Na}^+$  influx pathways, but other transporters may become increasingly important during altered conditions (e.g. acidosis or cell volume stress). Mitochondria also exhibit  $\text{Na}^+/\text{Ca}^{2+}$  antiporter and  $\text{Na}^+/\text{H}^+$  exchange activity that are important in mitochondrial function. These coupled fluxes of  $\text{Na}^+$  with  $\text{Ca}^{2+}$ ,  $\text{H}^+$  and  $\text{HCO}_3^-$  make the detailed understanding of  $[\text{Na}^+]_i$  regulation pivotal to the understanding of both cardiac excitation–contraction coupling and pH regulation. The  $\text{Na}^+/\text{K}^+$ -ATPase is the main route for  $\text{Na}^+$  extrusion from cells and  $[\text{Na}^+]_i$  is a primary regulator under physiological conditions.  $[\text{Na}^+]_i$  is higher in rat than rabbit ventricular myocytes and the reason appears to be higher  $\text{Na}^+$  influx in rat with a consequent rise in  $\text{Na}^+/\text{K}^+$ -ATPase activity (rather than lower  $\text{Na}^+/\text{K}^+$ -ATPase function in rat). This has direct functional consequences. There may also be subcellular  $[\text{Na}^+]_i$  gradients locally in ventricular myocytes and this may also have important functional implications. Thus, the balance of  $\text{Na}^+$  fluxes in heart cells may be complex, but myocyte  $\text{Na}^+$  regulation is functionally important and merits focused attention as in this issue.

© 2003 European Society of Cardiology. Published by Elsevier Science B.V. All rights reserved.

Keywords: Myocytes; Na/Ca-exchanger; Na/H-exchanger; Na/K-pump; Na-channel

## 1. General aspects of cardiac $\text{Na}^+$ regulation

Intact cells maintain a large electrochemical  $[\text{Na}^+]$  gradient across the plasma membrane. While extracellular  $[\text{Na}^+]$  ( $[\text{Na}^+]_o$ ) is ~140 mM, intracellular free  $[\text{Na}^+]$  ( $[\text{Na}^+]_i$ ) is normally 4–16 mM. In excitable cells, the energy stored in the transmembrane  $\text{Na}^+$  gradient provides the basis for fast electrical signaling, i.e. propagation of action potentials in neurons and muscles. Many cells utilize the electrochemical  $\text{Na}^+$  gradient to couple ener-

getically unfavorable transmembrane solute flow to  $\text{Na}^+$  transport (secondary active transport). Examples include  $\text{Na}^+/\text{neurotransmitter}$ ,  $\text{Na}^+/\text{glucose}$  and  $\text{Na}^+/\text{amino acids}$  cotransporters as well as various  $\text{Na}^+/\text{ion}$  co- and counter-transporters. The  $[\text{Na}^+]_i$  also plays an important role in regulating the mitochondrial pH,  $[\text{Na}^+]$  and  $[\text{Ca}^{2+}]$ , as a substrate for mitochondrial  $\text{Na}^+/\text{H}^+$  and  $\text{Na}^+/\text{Ca}^{2+}$  exchangers.

Let us consider (Fig. 1A) the free energy of the electrochemical  $\text{Na}^+$  gradient  $\Delta G_{\text{Na}} = RT \ln([\text{Na}^+]_i/[\text{Na}^+]_o) + zFE_m$ , where the first term is the chemical energy while the second is the electrical energy ( $R$  is the

\*Corresponding author. Tel.: +1-708-216-1018; fax: +1-708-216-6308.

 E-mail address: [dbers@lumc.edu](mailto:dbers@lumc.edu) (D.M. Bers).

Time for primary review 28 days.



energies in the  $\text{Na}^+$  and NCX gradients can change with conditions and this will be addressed in more detail below (see  $\text{Na}^+/\text{Ca}^{2+}$  exchange section below).

While  $\text{Na}^+$  is analogous to  $\text{Ca}^{2+}$  in the steep electrochemical gradient favoring ion entry, cells seem to use  $\text{Na}^+$  and  $\text{Ca}^{2+}$  fluxes differently.  $\text{Ca}^{2+}$  can carry a major depolarizing current in cellular excitation, but in addition free intracellular  $[\text{Ca}^{2+}]$  ( $[\text{Ca}^{2+}]_i$ ) often changes by a factor of  $\sim 10$  during activation in many cell types (from  $\sim 100$  nM to  $\sim 1$   $\mu\text{M}$ , often in less than 100 ms). The large change in  $[\text{Ca}^{2+}]_i$  allows  $[\text{Ca}^{2+}]_i$  to function as a remarkably ubiquitous second messenger in regulating processes such as contraction, secretion and transcription. However, while the  $\text{Na}^+$  gradient is used directly for electrical signaling via  $\text{Na}^+$  current, changes in  $[\text{Na}^+]_i$  are typically small requiring many seconds to minutes to rise by even 10%. This makes  $[\text{Na}^+]_i$  itself a poor candidate for the sort of rapid dynamic regulation attributed to  $[\text{Ca}^{2+}]_i$ . However, the high concentration of  $\text{Na}^+$  (in the mM range) allows it to readily participate in quantitatively large coupled transport fluxes. This is important for both the transport of ions across membranes of many cell types, but is also important in driving the uphill transport of important cellular substrates such as glucose, amino acids and neurotransmitters.

In the steady-state,  $[\text{Na}^+]_i$  is determined by the balance between  $\text{Na}^+$  influx and efflux. There are several pathways for  $\text{Na}^+$  entry into cardiac cells (Table 1 and Fig. 1B). Voltage-gated  $\text{Na}^+$  channels are responsible for the upstroke of action potentials. NCX generally uses  $\text{Na}^+$  influx to extrude  $\text{Ca}^{2+}$ , and is the main mechanism for  $\text{Ca}^{2+}$  extrusion during relaxation.  $\text{Na}^+/\text{H}^+$  exchange (NHE) extrudes  $\text{H}^+$  in exchange for  $\text{Na}^+$  and is critical in cellular pH homeostasis. Another important acid extruding transport is the  $\text{Na}^+/\text{HCO}_3^-$  cotransporter (NBC). There is also a  $\text{Na}^+/\text{K}^+/\text{2Cl}^-$  cotransporter (NKCC) important in volume regulation, and a  $\text{Na}^+/\text{Mg}^{2+}$  exchanger (NMgX) that

is involved in extruding  $\text{Mg}^{2+}$ .  $\text{Na}^+$  entering the cells through these mechanisms is then extruded by the  $\text{Na}^+/\text{K}^+$  pump. The pump utilizes energy derived from the hydrolysis of ATP to exchange three internal  $\text{Na}^+$  for two external  $\text{K}^+$  ions and thus maintains the transmembrane  $[\text{Na}^+]$  gradient. Intracellular buffering is important in the regulation of many intracellular ions, including  $\text{Ca}^{2+}$  (100:1),  $\text{Mg}^{2+}$  ( $\sim 100$ :1) and pH ( $>1000$ :1). Although data regarding intracellular  $\text{Na}^+$  buffering are sparse, we recently measured very low  $\text{Na}^+$  buffering capacity ( $\sim 1.3$ ) in rabbit ventricular myocytes by measuring simultaneously  $[\text{Na}^+]_i$  and integrated  $\text{Na}^+/\text{K}^+$  pump current during  $[\text{Na}^+]_i$  decline upon abrupt pump activation [1]. However, this low global  $\text{Na}^+$  buffering capacity does not preclude local subsarcolemmal  $\text{Na}^+$  buffering which may exist (see below).

Resting  $[\text{Na}^+]_i$  in heart cells is in the range of 4–8 mM for most mammalian species [2–7] and much higher (10–15 mM) in rat and mouse [4–9]. This interspecies difference is rather intriguing, as higher resting  $[\text{Na}^+]_i$  might limit  $\text{Ca}^{2+}$  extrusion, altering cellular  $\text{Ca}^{2+}$  balance and also contributes to rest potentiation, seen in rat, mouse and some other cardiac muscle [7].  $[\text{Na}^+]_i$  increases during stimulation in a frequency dependent manner. This is because  $\text{Na}^+$  influx per unit time is higher due to more frequent activation of  $\text{Na}^+$  channels and NCX. Cook et al. [10] showed that there are also regional differences in the regulation of  $[\text{Na}^+]_i$  in rabbit left ventricle (higher in sub-epicardial than sub-endocardial myocytes) both at rest and during steady-state stimulation at 0.5 Hz. However, the expression of the  $\text{Na}^+/\text{K}^+$  pump and the pump current density are similar in the two regions [11]. This suggests that regional differences in  $[\text{Na}^+]_i$  regulation might arise from differences in  $\text{Na}^+$  influx.

Because of NCX, NHE and NBC,  $[\text{Na}^+]_i$  is centrally involved in controlling the  $[\text{Ca}^{2+}]_i$  and  $\text{pH}_i$ . Therefore,  $[\text{Na}^+]_i$  plays an important role in the heart, as both these

Table 1  
 $\text{Na}^+$  transport in cardiac cells

	Nickname	Transport and stoichiometry	Resting flux rate <sup>a</sup> (mM/min)	Inhibitors
<i>Na extrusion pathways</i>				
$\text{Na}^+/\text{K}^+$ -ATPase	$\text{Na}^+$ pump, $I_{\text{pump}}$	3 $\text{Na}^+$ :2 $\text{K}^+$ exchange	0.77 <sup>b</sup>	Cardiac glycosides
<i>Na influx pathways</i>				
$\text{Na}^+$ channel/current	$I_{\text{Na}}$	Uncoupled	0.14	Tetrodotoxin
$\text{Na}^+/\text{Ca}^{2+}$ exchanger <sup>c</sup>	NCX	3 $\text{Na}^+$ :1 $\text{Ca}^{2+}$ exchange <sup>d</sup>	0.28	$\text{Ni}^{2+}$
$\text{Na}^+/\text{H}^+$ exchanger	NHE	1 $\text{Na}^+$ :1 $\text{H}^+$ exchange	0.12	Amiloride, cariporide
$\text{Na}^+/\text{HCO}_3^-$ cotransporter	NBC	1 $\text{Na}^+$ :1 $\text{HCO}_3^-$ cotransport <sup>d</sup>	0.12	DIDS, SITS
$\text{Na}^+/\text{K}^+/\text{2Cl}^-$ cotransporter	NKCC	1 $\text{Na}^+$ :1 $\text{K}^+$ :2 $\text{Cl}^-$ cotransport	0.15	Furosemide, bumetanide
$\text{Na}^+/\text{Mg}^{2+}$ antiporter	NaMgX	2 $\text{Na}^+$ :1 $\text{Mg}^{2+}$ exchange	0.08	Imipramine

<sup>a</sup> Values are based in part on our measurements in rabbit ventricular myocytes [5] and some extrapolations from guinea-pig data [80,102] (see text for details).

<sup>b</sup> Determined in Ref. [5] for a  $[\text{Na}^+]_i$  of 5 mM.

<sup>c</sup> Depending on the internal and external  $\text{Na}^+$  and  $\text{Ca}^{2+}$  concentrations and the membrane potential, the  $\text{Na}^+/\text{Ca}^{2+}$  exchanger can also function as a  $\text{Na}^+$  extrusion pathway (see text for details).

<sup>d</sup> Stoichiometry is still a matter of debate (see text).

ions are important factors in excitation–contraction coupling (ECC) [12]. An increase in  $[\text{Na}^+]_i$  would shift the balance of fluxes on the NCX to favor more  $\text{Ca}^{2+}$  influx and less  $\text{Ca}^{2+}$  efflux, resulting in larger  $\text{Ca}^{2+}$  transients and therefore enhanced contractility. This is the likely mechanism of the inotropic effect of cardiac glycosides, which are specific inhibitors of the  $\text{Na}^+/\text{K}^+$  pump and have been used to enhance cardiac contractility in the treatment of congestive heart failure for more than 200 years. Indeed, relatively small changes of  $[\text{Na}^+]_i$  can have major effects on contractile force. In cardiac Purkinje fibers, force can double with  $\sim 1$  mM rise of  $[\text{Na}^+]_i$  [13]. In ventricular muscle, small increases in  $[\text{Na}^+]_i$  produce less percentage increase in force, probably because of a ceiling effect. That is, in rabbit ventricle at  $\sim 29^\circ\text{C}$  and 0.5 Hz, control twitches are already  $\sim 40\%$  of the maximum myofilament force [14], limiting the extent of further increase.

As Fig. 1B indicates there are many  $\text{Na}^+$  entry pathways, but the  $\text{Na}^+/\text{K}^+$ -ATPase is the main  $\text{Na}^+$  extrusion pathway. We will first consider  $\text{Na}^+/\text{K}^+$ -ATPase and then  $\text{Na}^+$  influx mechanisms.

## 2. $\text{Na}^+/\text{K}^+$ pump

### 2.1. $\text{Na}^+/\text{K}^+$ pump structure, isoforms and expression in the heart

The  $\text{Na}^+/\text{K}^+$  pump is a member of the P-type ATPase pumps. The reaction mechanism of these ATPases is based on the formation of a phosphorylated intermediate. Accompanying the phosphorylation–dephosphorylation process, P-type ATPases bind, occlude and transport ions by cycling between two different conformations, called E1 and E2 [15]. The  $\text{Na}^+/\text{K}^+$ -ATPase has two major subunits:  $\alpha$  and  $\beta$  (for a review, see Ref. [16]). The  $\alpha$  subunit was first cloned by Shull et al. [17] and Kawakami et al. [18], has a molecular weight of  $\sim 110$  kDa and contains the binding sites for ATP,  $\text{Na}^+$ ,  $\text{K}^+$  and cardiac glycosides (specific inhibitors of the enzyme). The smaller  $\beta$  subunit ( $\sim 50$  kDa) modulates the ATPase activity and is important in the proper membrane insertion of the pump. A third, smaller ( $\sim 12$  kDa) protein ( $\gamma$  subunit) has also been found in various tissues [19] but its physiological function is not yet known. Four  $\alpha$  ( $\alpha_1$ – $\alpha_4$ ) and three  $\beta$  ( $\beta_1$ – $\beta_3$ ) subunits of the  $\text{Na}^+/\text{K}^+$ -ATPase have been identified. The  $\alpha_1$ – $\alpha_3$  isoforms are expressed in a variety of tissues, whereas the  $\alpha_4$  isoform has only been detected in rat testis [20]. Any  $\alpha\beta$  combination results in a functional pump.

The  $\alpha_1$  isoform is present in the cardiac tissue of all species studied, but there is marked variation of  $\alpha_2$  and  $\alpha_3$  subunit expression among species. All three  $\alpha$ -isoforms are present in the human heart [21–23], whereas  $\alpha_1$  and  $\alpha_3$  isoforms are expressed in dog [24,25] and ferret [26]. The  $\alpha_1$  isoform is predominant in rabbit [11] and guinea-pig

[23] heart, although small amounts of  $\alpha_3$  [27] and  $\alpha_2$  [28], respectively, have also been reported. In the rat, the  $\alpha_1$  and  $\alpha_3$  isoforms are expressed in fetal and neonatal hearts and the  $\alpha_3$  isoform is replaced by the  $\alpha_2$  isoform early in development [29,30]. Interestingly, the reverse switch (from  $\alpha_2$  to  $\alpha_3$ ) occurs in hypertrophied or failing rat heart [31,32]. The  $\beta_1$  isoform is the only  $\beta$  subunit appreciably expressed in the human heart [22], although a recent report indicated that  $\beta_3$  is also present [33].

Different  $\text{Na}^+/\text{K}^+$ -ATPase isoforms have different glycosides and  $[\text{Na}^+]_i$  sensitivity. In the rat,  $\alpha_1$  is  $\sim 100$  times more resistant to ouabain than  $\alpha_2$  and  $\alpha_3$ . In rabbit, pig, dog and human, the  $\alpha_1$  isoform is much more sensitive to ouabain than in rat (for a review, see Ref. [16]), therefore the differences in glycosides affinity are not as marked. Indeed, it has been recently shown [34] that the affinity of all three human  $\alpha$  subunit isoforms for ouabain is similar ( $\sim 18$  nM). Expression of  $\text{Na}^+/\text{K}^+$ -ATPase is higher in ventricle than atrium [22]. In ventricular myocytes,  $\text{Na}^+/\text{K}^+$  pumps are located in both peripheral sarcolemma and T-tubules [23]. In the rat, the  $\alpha_1$  isoform is preferentially distributed in T-tubules, whereas  $\alpha_2$  and  $\beta_1$  are homogeneously distributed in the T-tubules and peripheral sarcolemma [23]. The level of expression of different isoforms and/or their cellular localization could have important physiological consequences. James et al. [35] studied the phenotypes of mouse hearts with genetically reduced levels of  $\alpha_1$  or  $\alpha_2$  isoforms. They found that heterozygous  $\alpha_2$  hearts have increased  $\text{Ca}^{2+}$  transients and contractility whereas the opposite happens for the  $\alpha_1$  heterozygotes. Furthermore, inhibition of the  $\alpha_2$  isoform with ouabain increased the contractility of heterozygous  $\alpha_1$  hearts. These results might indicate a specific role for the  $\alpha_2$  isoform as a regulator of  $\text{Ca}^{2+}$  in the mouse heart, for example by affecting the function of the Na/Ca exchange. This can happen if the  $\alpha_2$  isoforms are preferentially located in the dyads. This is indeed the case in smooth muscle where the low ouabain-affinity  $\alpha_1$ -isoform is ubiquitously distributed, but the higher affinity  $\alpha_2$ - and  $\alpha_3$ -isoforms are preferentially localized in regions overlying the SR [36].

### 2.2. Ion transport characteristics of the $\text{Na}^+/\text{K}^+$ pump

The  $\text{Na}^+/\text{K}^+$ -ATPase transports three  $\text{Na}^+$  ions out and two  $\text{K}^+$  ions into the cell using the energy of one ATP molecule, and thus moves out one net charge per cycle. Ion transport by the  $\text{Na}^+/\text{K}^+$  pump has a functional reversal potential which depends on both intracellular and extracellular  $[\text{Na}^+]$  and  $[\text{K}^+]$ , as well as the free energy of intracellular ATP hydrolysis ( $\Delta G_{\text{ATP}}$ ). Under normal conditions, the reversal potential has been estimated to be about  $-180$  mV [37], such that  $\text{Na}^+/\text{K}^+$  pump current ( $I_{\text{pump}}$ ) and  $\text{Na}^+$  transport are outward over the whole physiological range. The ATP concentration for half-maxi-

mal activation of the cardiac  $\text{Na}^+/\text{K}^+$  pump is in the range of 80–150  $\mu\text{M}$  [38,39], therefore under control conditions ATP is not rate limiting for the pump (normal ATP levels in cardiac cells are 5–10 mM). However, this can change as [ATP] declines during ischemia or metabolic inhibition, and the simultaneous rise in [ADP] and  $[\text{P}_i]$  also contribute to a reduced  $\Delta G_{\text{ATP}}$  available for transport. Such a reduction in  $\Delta G_{\text{ATP}}$  would also reduce the  $[\text{Na}^+]$  and  $[\text{K}^+]$  gradients that the pump can generate. However, during short-term metabolic inhibition glycolysis may regenerate ATP near the  $\text{Na}^+/\text{K}^+$ -ATPase, making the pump less directly dependent on oxidative phosphorylation [40].

The main physiological regulators of the  $\text{Na}^+/\text{K}^+$  pump are internal  $\text{Na}^+$  and external  $\text{K}^+$ . The  $[\text{Na}^+]_i$  for half-maximal pump activation ( $K_m$ ) in the heart varies widely with the internal and external ionic conditions, in the range of 8–22 mM (for a review, see Ref. [41]). Intracellular  $\text{K}^+$  competes with  $\text{Na}^+$  for binding to the enzyme at the cytoplasmic surface and results in reduced  $[\text{Na}^+]_i$ -sensitivity of the pump [42]. The activating  $K_m$  for extracellular  $\text{K}^+$ , in the presence of normal external  $[\text{Na}^+]$ , is 1–2 mM [41], therefore the pump is  $\sim 70\%$  saturated with respect to external  $\text{K}^+$  at a normal concentration of 4 mM. External  $\text{Na}^+$  and  $\text{K}^+$  compete for common binding sites to the  $\text{Na}^+/\text{K}^+$ -ATPase, therefore the  $K_m$  for pump activation by external  $\text{K}^+$  is appreciably lower in  $\text{Na}^+$ -free conditions [43]. The absence of external  $\text{Na}^+$  also renders  $I_{\text{pump}}$  voltage insensitive [43]. With normal  $\text{Na}^+$  outside, the  $E_m$ -dependence of  $I_{\text{pump}}$  in ventricular myocytes is sigmoidal in shape with a steep positive slope between  $-100$  and  $0$  mV and nearly no voltage dependence of  $I_{\text{pump}}$  at positive potentials [44] (for a review, see Ref. [45]).

As mentioned above, multiple  $\text{Na}^+/\text{K}^+$ -ATPase isoforms exist in cardiac cells from most species, and they might differ functionally because of differential specific intracellular localization, regulation or kinetic characteristics. The  $[\text{Na}^+]_i$ -dependence of the three rat  $\alpha$ -subunit isoforms has been studied in transfected cells [16,46]. When transfected into insect cells, the apparent affinity for intracellular  $\text{Na}^+$  varies in the order  $\alpha_2 > \alpha_1 > \alpha_3$  [16] whereas in HeLa cells the order seems to be  $\alpha_1 > \alpha_2 > \alpha_3$  [46]. This difference might be due to the different method used to determine the pump activity ( $\text{Na}^+/\text{K}^+$ -ATPase activity vs. the rate of  $\text{Na}^+$  extrusion from intact cells). However, the common point is that  $\alpha_3$  isoform has a much lower  $\text{Na}^+$ -affinity ( $K_m \sim 30$  mM) than  $\alpha_1$  or  $\alpha_2$ , making it less active at physiological  $[\text{Na}^+]_i$ , perhaps serving as a ‘safety’ mechanism in conditions of  $\text{Na}^+$  overload. The  $\alpha_3$  isoform also has a lower  $[\text{K}^+]_o$  affinity [16].

How much  $\text{Na}^+$  is extruded by the  $\text{Na}^+/\text{K}^+$ -ATPase to maintain steady-state  $[\text{Na}^+]_i$ ? We measured [5] the  $[\text{Na}^+]_i$ -dependence of the  $\text{Na}^+/\text{K}^+$  pump-mediated  $\text{Na}^+$  efflux in rat and rabbit ventricular myocytes (Fig. 2A). There is little difference in the  $\text{Na}^+/\text{K}^+$  pump rate for  $[\text{Na}^+]_i$  below 11 mM. However,  $\text{Na}^+/\text{K}^+$ -ATPase maximum rate ( $V_{\text{max}}$ ) was nearly twice as high in rat and the half-

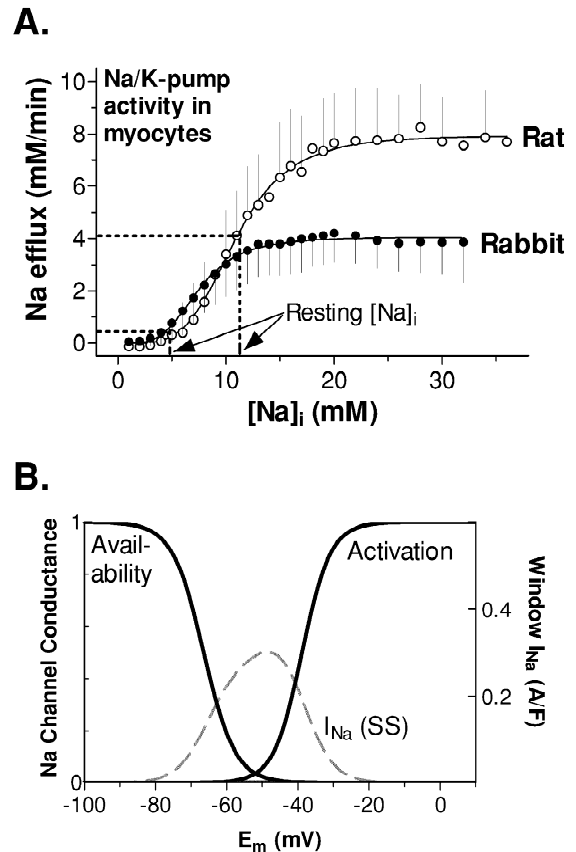


Fig. 2. (A) The  $[\text{Na}^+]_i$ -dependence of  $\text{Na}^+/\text{K}^+$  pump-mediated  $\text{Na}^+$  efflux in rat and rabbit ventricular myocytes. Cells were first  $\text{Na}^+$ -loaded by inhibiting the  $\text{Na}^+/\text{K}^+$  pump in the absence of external  $\text{K}^+$ . Then, the pump was re-activated with 4 mM  $\text{K}^+$  and we monitored the time course of  $[\text{Na}^+]_i$  decline. The rate of  $[\text{Na}^+]_i$  decline ( $-d[\text{Na}^+]_i/dt$ ) was calculated at each  $[\text{Na}^+]_i$ . The solid lines represent the fit with a Hill expression. Replotted from Ref. [5]. (B) Steady-state  $E_m$ -dependence of  $I_{\text{Na}}$  activation, inactivation (or availability) and window current.

activation by  $\text{Na}^+$  ( $K_m(\text{Na})$  (was higher in rat) 10 vs. 7 mM). The  $V_{\text{max}}$  values may indicate higher pump protein expression levels in rat versus rabbit. We speculate that this might be a cellular adaptation to a chronically higher  $[\text{Na}^+]_i$ , and there is precedent for such  $[\text{Na}^+]_i$ -dependent upregulation of  $\text{Na}^+/\text{K}^+$ -ATPase expression levels [47]. Fig. 2A indicates that at rest, when  $[\text{Na}^+]_i$  is 4.5 mM in rabbit and 11.1 mM in rat [5], the  $\text{Na}^+/\text{K}^+$  pump is only running at  $\sim 15\%$  of  $V_{\text{max}}$  in rabbit ventricle versus  $\sim 60\%$  in rat. Therefore rabbit cells might have a greater reserve to cope with an enhanced  $\text{Na}^+$  influx brought about by higher stimulation frequency or by pathological conditions. The rate of  $\text{Na}^+$  efflux in rat at the higher measured resting  $[\text{Na}^+]_i$  is higher than the resting  $\text{Na}^+/\text{K}^+$ -pump rate in rabbit ventricular myocytes (Fig. 2A). Since  $\text{Na}^+$  efflux must equal  $\text{Na}^+$  influx at the steady state, this means that resting  $\text{Na}^+$  influx must also be higher in rat than rabbit ventricular myocyte. In the following, we will discuss pathways that contribute to this  $\text{Na}^+$  influx.

### 3. Pathways for Na<sup>+</sup> influx

#### 3.1. Voltage-gated Na<sup>+</sup> channels

Voltage-gated Na<sup>+</sup> channels are activated by depolarization and are responsible for the rapid upstroke of the cardiac action potential (AP). Once threshold depolarization for an AP is reached, the opening of Na<sup>+</sup> channels leads to further depolarization, which activates additional Na<sup>+</sup> channels and depolarization, etc. This positive feedback creates a very rapid depolarization toward the electrochemical potential of Na<sup>+</sup>. Depolarization stops, in part because Na<sup>+</sup> channels inactivate, i.e. under sustained depolarization, the amplitude of Na<sup>+</sup> current ( $I_{Na}$ ) decreases.  $I_{Na}$  inactivation effectively switches off Na<sup>+</sup> conductance within a few milliseconds or less (fast inactivation).

Voltage-gated Na<sup>+</sup> channels are composed of a pore-forming  $\alpha$  subunit and auxiliary  $\beta$  subunits. Ten genes encoding  $\alpha$  subunits have been identified and nine have been functionally expressed. The  $\alpha$  subunit consists of four repeat domains (I–IV), each containing six transmembrane segments (S1–S6) and one membrane reentrant domain, connected by internal and external polypeptide loops [48]. The S4 segments contain four to eight positively charged residues, which serve as voltage sensors. An outward movement of these charges under depolarization underlies the activation of the channel [49]. Inactivation is mediated by the short intracellular loop connecting domains III and IV. One  $\alpha$  subunit is associated with one or two auxiliary  $\beta$  subunits,  $\beta_1$ ,  $\beta_2$  or  $\beta_3$ . These auxiliary subunits modulate channel gating, interact with extracellular matrix and play a role as cell adhesion molecules [50]. The primary cardiac  $\alpha$  subunit isoform (Na<sub>v</sub>1.5) is much less sensitive to inhibition by TTX ( $K_{0.5} \sim 2 \mu\text{M}$ ) and is more sensitive to Cd<sup>2+</sup> block than neuronal or skeletal muscle Na<sup>+</sup> channels.

Fig. 2B shows the  $E_m$ -dependence of Na<sup>+</sup> channels activation and availability (or steady-state inactivation).  $I_{Na}$  activation and availability curves overlap such that there is almost no steady state availability when  $E_m$  is held at values where activation is appreciable. This ensures that activated Na<sup>+</sup> channels inactivate nearly completely whenever activated by depolarization. Na<sup>+</sup> channels require repolarization to recover from inactivation before another AP can occur. This is a main cause of the electrical refractory period. Recovery of  $I_{Na}$  requires that the membrane be repolarized to near the diastolic level for a finite period of time ( $\tau \sim 10$  ms at  $-100$  mV, 30 ms at  $-80$  mV or 100 ms at  $-72$  mV) before the cell is able to fire another AP. Thus Na<sup>+</sup> channels do not recover very rapidly until repolarization is nearly complete. In this way the long AP contributes to limiting the ability of the cell to respond to an early depolarization. Besides these fast inactivating Na<sup>+</sup> channels, there are indications that a slowly inactivating, persistent Na<sup>+</sup> current ( $I_{Na,slow}$ ) might

also be present in cardiac cells [51,52]. This persistent Na<sup>+</sup> current is more sensitive to block by TTX, is activated at more negative potentials and has an amplitude of  $\sim 0.5\%$  of the peak transient  $I_{Na}$ . It has been shown that  $I_{Na,slow}$  has a more prominent contribution to  $I_{Na}$  in heart failure and might be partly responsible for the prolongation of the AP [52,53].

As shown in Fig. 2B, there is a very small window at about  $-52$  mV where both channel availability and activation are  $\sim 3.5\%$ . This would produce a steady state ‘window current’ with a conductance of  $\sim 0.1\%$  of maximum. Considering a peak  $I_{Na}$  of 360 pA/pF and a surface to volume ratio of 6.4 pF/pL<sub>cyt</sub> [54], this steady current (0.3 A/F) would result in a significant Na<sup>+</sup> influx of 1.4 mM/min. At a resting  $E_m$  of  $-80$  mV this window  $I_{Na}$  would be 10–30 times smaller, but would be consistent with our measurements of tetrodotoxin (TTX) sensitive resting Na<sup>+</sup> influx in rabbit ventricular myocytes at 23 and 37 °C (0.14–0.18 mM/min [5,55]). This would require a window  $I_{Na}$  of  $\sim 0.01\%$  of maximum. This and the steepness of the activation and availability curves emphasizes that small shifts in activation or inactivation properties could lead to substantial sustained Na<sup>+</sup> influx via window  $I_{Na}$  at relatively negative  $E_m$ .

During the cardiac AP upstroke  $I_{Na}$  is very large, but very brief. This results in an additional Na<sup>+</sup> influx associated with each AP. Fig. 3C and D shows  $I_{Na}$  and the Na<sup>+</sup> influx via Na<sup>+</sup> channels during a typical AP, respectively. Fig. 3D indicates that  $\sim 8 \mu\text{M}$  Na<sup>+</sup> enters the cell via  $I_{Na}$  during each AP (6–15  $\mu\text{M}$  is probably a reasonable range). For a cell contracting at 1 Hz, this means that phasic Na<sup>+</sup> channel activation contributes  $\sim 0.5$  mM/min to the rate of Na<sup>+</sup> influx. This is surprisingly only about a 3-fold increase over the resting  $I_{Na}$  influx.

#### 3.2. Na<sup>+</sup>/Ca<sup>2+</sup> exchange

Na<sup>+</sup>/Ca<sup>2+</sup> exchange is the major pathway for Ca<sup>2+</sup> extrusion from cardiac myocytes. The mammalian NCX forms a multigene family of homologous proteins comprising three isoforms: NCX1, NCX2 and NCX3 (for reviews, see Refs. [56–58]). These isoforms share  $\sim 70\%$  amino acid identity in the overall sequences and thus presumably have a very similar molecular structure. NCX1 is the first NCX cloned and is highly expressed in cardiac muscle and brain and to a lesser extent in many other tissues. NCX2 and NCX3 are expressed in a few tissues, such as brain, but their molecular properties and functions have been less well studied.

The cardiac NCX1 consists of 970 amino acids (110 kDa). Approximately half of the NCX1 protein constitutes transmembrane domains, whereas the remaining half ( $\sim 550$  amino acids) forms a large domain exposed on the cytoplasm. The latter domain does not appear to be required for the transport function of NCX1, because a mutant lacking most of it still retains exchange activity

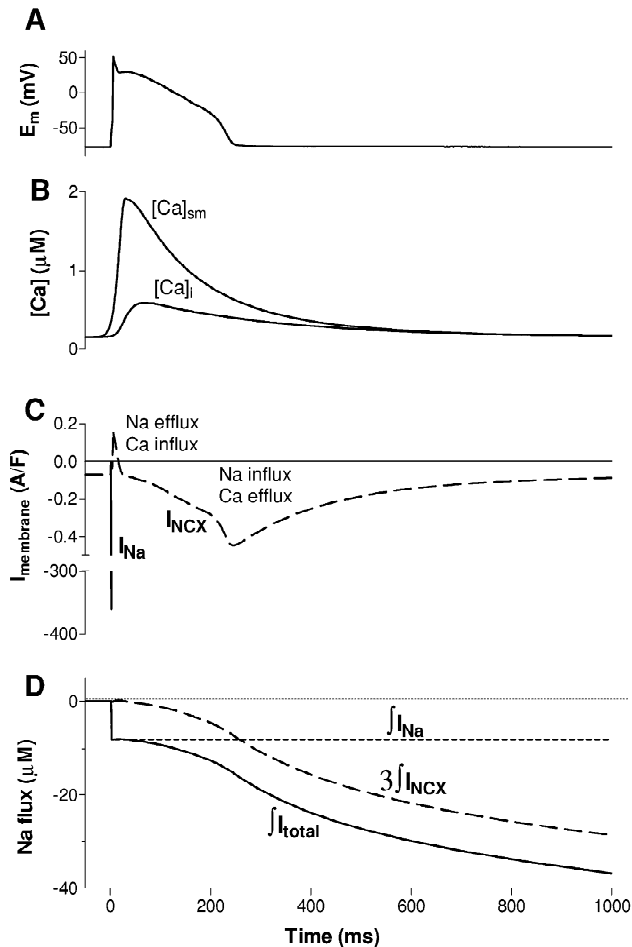


Fig. 3. Calculated  $I_{Na}$  and  $I_{NCX}$  mediated  $Na^+$  influx in a ventricular myocyte contracting at 1 Hz. (A) Typical action potential for rabbit ventricular myocytes. (B)  $[Ca^{2+}]_i$  and  $[Ca^{2+}]_{sm}$  transients during an AP.  $[Ca^{2+}]_{sm}$  was calculated from the measured  $[Ca^{2+}]_i$  transient as described by Weber et al. [72]. (C) Calculated density of  $Na^+$  current via  $Na^+$  channels ( $I_{Na}$ ) and density of NCX current ( $I_{NCX}$ ) during an AP using the  $I_{NCX}$  equation of Weber et al. [73]. (D) Net  $Na^+$  fluxes via  $Na^+$  channels ( $\int I_{Na}$ ) and NCX ( $3\int I_{NCX}$ ), as well as the total  $Na^+$  flux ( $\int I_{total}$ ) during the AP.

[59]. There were originally thought to be 11 transmembrane domains and a very large cytoplasmic hydrophilic domain [60]. However, new topological data suggest that there are only nine transmembrane spans [61] and a large hydrophilic loop between TMs 5 and 6, with N- and C-termini located on the external and internal sides, respectively. The N-terminal and C-terminal halves of the membrane domain contain two internal repeat sequences of ~40 amino acids, which are designated the  $\alpha_1$  and  $\alpha_2$  repeats. These repeat sequences are conserved in all members of the NCX family as well as in related cation exchangers, and are now thought to be at or near the ion translocation pore. Many details of the NCX1 structure are unknown, including the ion transport pathway, the requirement of the oligomeric protein structure for the function, and changes in the conformation of the exchanger associ-

ated with ion transport. The density of NCX1 in the sarcolemma of guinea pig ventricular myocytes has been estimated to be 250–400 NCX/ $\mu m^2$  [62].

NCX is generally believed to transport three  $Na^+$  ions in exchange for one  $Ca^{2+}$  (for a review, see Ref. [56]), thus one net charge is transported per cycle. However, some recent studies indicate a 4:1 [63,64] or, under extremely acidic conditions, a 2:1 stoichiometry [65]. The direction and amount of ion fluxes through NCX depend on the  $[Na^+]$  and  $[Ca^{2+}]$  on both sides of the membrane, as well as on  $E_m$ . If there is more energy in the inward  $Na^+$  gradient (for three  $Na^+$  ions) than in the inward  $Ca^{2+}$  gradient (for one  $Ca^{2+}$  ion),  $Ca^{2+}$  extrusion will be favored. That is:  $n(E_{Na} - E_m) > 2(E_{Ca} - E_m)$ , where  $n$  is the coupling ratio and  $E_{Ca}$  and  $E_{Na}$  are the thermodynamic equilibrium potentials for  $Ca^{2+}$  and  $Na^+$ . Then, the  $E_m$  value at which the gradients are exactly equal is the reversal potential ( $E_{Na/Ca}$ ) of the  $I_{NCX}$ . Hence,  $E_{Na/Ca} = (nE_{Na} - 2E_{Ca})/(n - 2)$ . When  $E_m$  is more positive than  $E_{Na/Ca}$ , outward  $I_{NCX}$  is favored. In other words,  $Ca^{2+}$  entry/ $Na^+$  exit via the exchanger is favored for  $E_m > E_{Na/Ca}$  and  $Ca^{2+}$  extrusion/ $Na^+$  entry is favored (inward  $I_{NCX}$ ) when  $E_m < E_{Na/Ca}$ . For the normally accepted  $n=3$  and typical values of  $E_{Na}=70$  mV and  $E_{Ca}=125$  mV,  $E_{Na/Ca}=-40$  mV. Because the resting membrane potential (~−80 mV) is more negative than  $E_{Na/Ca}$ , the exchanger will work in  $Ca^{2+}$  extrusion/ $Na^+$  influx mode in resting myocytes. During the action potential, NCX briefly works in  $Ca^{2+}$  entry/ $Na^+$  exit mode, i.e.  $E_m > E_{Na/Ca}$  (see Fig. 3C and discussion below).

Besides being transport substrates, intracellular  $Ca^{2+}$  and  $Na^+$  exert important modulatory effects on NCX activity [57,58]. Binding of intracellular  $Ca^{2+}$  to a high affinity site located in the central hydrophilic loop activates the exchanger ( $[Ca^{2+}]_i$ -dependent activation). It should be appreciated that this allosteric  $Ca^{2+}$ -regulatory site is distinct from the catalytic or  $Ca^{2+}$ -transport site. While  $K_m(Ca)$  values from 22 to 600 nM have been reported for this allosteric regulation by  $[Ca^{2+}]_i$ , a recent study by Weber et al. [66] found a physiologically relevant  $K_m(Ca)$  of 125 nM in intact ferret ventricular myocyte during dynamic  $[Ca^{2+}]_i$  changes. This allosteric  $Ca^{2+}$ -activation was rapid (within tens of ms) and so it is probably important physiologically during beat-to-beat changes in cellular  $Ca^{2+}$ . There is also an inhibitory regulation at high  $[Na^+]_i$  [67]. NCX inactivates in a time and  $[Na^+]_i$ -dependent manner. This  $[Na^+]_i$ -dependent inactivation could prevent excess  $Ca^{2+}$  influx and cellular  $Ca^{2+}$  overload under conditions of high  $[Na^+]_i$ , where net  $Ca^{2+}$  influx might be strongly favored. However, the very high  $[Na^+]_i$  required to observe  $Na^+$ -dependent inactivation of  $I_{NCX}$  makes this regulation unlikely to be very important in the physiological modulation of NCX.

NCX exhibits relatively low activity in intact myocytes at rest (partly because  $[Ca^{2+}]_i$  is low). Therefore,  $Na^+$  influx via NCX is rather low in quiescent cells. We

measured the rate of Ni-sensitive  $[\text{Na}^+]_i$  influx upon abrupt  $\text{Na}^+/\text{K}^+$  pump inhibition in resting rabbit and rat ventricular myocytes. Resting  $\text{Na}^+$  influx via NCX was 0.28 mM/min in rabbit ventricular myocyte (Fig. 4A) and 0.64 mM/min in rat. From a functional standpoint, this basal rate of  $\text{Na}^+$  influx via NCX would extrude 1.5 and 3.5  $\mu\text{M}$   $\text{Ca}^{2+}$ /s in rabbit and rat, respectively. This is on the order of estimates of resting  $\text{Ca}^{2+}$  leak into ventricular myocytes (0.5–5  $\mu\text{M}$ /s; [68–70]). There is also a sarcolemmal  $\text{Ca}^{2+}$ -ATPase, and it is reasonable to infer that resting  $\text{Ca}^{2+}$  extrusion (to match this inward resting  $\text{Ca}^{2+}$  leak) via NCX and the sarcolemmal  $\text{Ca}^{2+}$ -ATPase are on

the same order of magnitude [70]. Of course NCX uses the  $[\text{Na}^+]$  electrochemical gradient (rather than ATP) to extrude  $\text{Ca}^{2+}$ , but the energy still comes from ATP via  $\text{Na}^+/\text{K}^+$ -ATPase.

It is not clear why there is higher  $\text{Na}^+$  influx via NCX in rat (vs. rabbit) myocytes, especially considering that  $[\text{Na}^+]_i$  is higher in rat. The density of outward NCX current upon  $[\text{Na}^+]_o$  removal is higher in rat than rabbit [71], so if that holds for inward NCX current as well that may provide a partial explanation.  $\text{Ca}^{2+}$  leak into rat myocytes might also be higher (which would require more  $\text{Na}^+$  influx via NCX). Resting SR  $\text{Ca}^{2+}$  spark frequency is also higher in rat versus rabbit [72], and the resulting high local  $[\text{Ca}^{2+}]_i$  may drive local  $\text{Ca}^{2+}$  extrusion and  $\text{Na}^+$  influx via NCX.

NCX function during the AP is complicated because  $[\text{Ca}^{2+}]_i$  and  $E_m$  change dramatically. This changes the reversal potential, kinetic and allosteric factors. There are also spatial gradients of  $[\text{Ca}^{2+}]_i$  near the sarcolemma which complicate this picture [73]. Fig. 3 shows  $I_{\text{NCX}}$  (panel C) and the  $\text{Na}^+$  flux via NCX (derived by integrating  $I_{\text{NCX}}$  and assuming a 3:1 stoichiometry, panel D) expected during an AP. Throughout most of the AP there is net  $\text{Na}^+$  influx ( $\text{Ca}^{2+}$  efflux) via NCX, except for a brief period early in the AP before  $[\text{Ca}^{2+}]_i$  has risen enough to cause  $\text{Ca}^{2+}$  extrusion. During each AP and  $\text{Ca}^{2+}$  transient NCX brings in  $\sim 32 \mu\text{M}$   $[\text{Na}^+]_i$ . Again, this  $\text{Na}^+$  influx is required to extrude the  $\sim 10 \mu\text{M}$   $\text{Ca}^{2+}$  which enters the cell via  $\text{Ca}^{2+}$  current during each AP (on a 3  $\text{Na}^+$ :1  $\text{Ca}^{2+}$  NCX). For a cell contracting at 1 Hz, this means that NCX contributes  $\sim 1.9 \text{ mM/min}$  to the rate of  $\text{Na}^+$  influx (about seven times higher than the resting  $\text{Na}^+$  influx rate via NCX). As can be seen from Fig. 3, this  $\text{Na}^+$  entry is more distributed over the course of the AP versus  $I_{\text{Na}}$ . Figs. 3 and 4 also show that, quantitatively,  $\text{Na}^+$  influx via NCX is considerably higher (three to four times) than that which occurs via  $\text{Na}^+$  channels.

As mentioned above, NCX is reversible and can also be a  $\text{Na}^+$  extrusion mechanism (using the large energy in the  $\text{Ca}^{2+}$  electrochemical gradient). However, this is unlikely to be a quantitatively important function under normal conditions. This can be appreciated by Fig. 3C where only a very small  $\text{Na}^+$  efflux occurs very early during the AP. This situation can change during heart failure where lower  $\text{Ca}^{2+}$  transient amplitude, higher  $[\text{Na}^+]_i$  and prolonged AP can all favor greater  $\text{Na}^+$  extrusion (and  $\text{Ca}^{2+}$  influx) via NCX [55]. On the other hand, whatever  $\text{Ca}^{2+}$  enters via NCX during the AP must also be extruded by NCX during the diastolic interval, making net  $\text{Na}^+$  extrusion via NCX negligible. Thus, NCX is probably not very important as a  $\text{Na}^+$  extrusion mechanism.

### 3.3. $\text{Na}^+/\text{H}^+$ exchange

Another  $\text{Na}^+$  influx pathway in cardiac cells is the  $\text{Na}^+/\text{H}^+$  exchanger (NHE), which is important in the

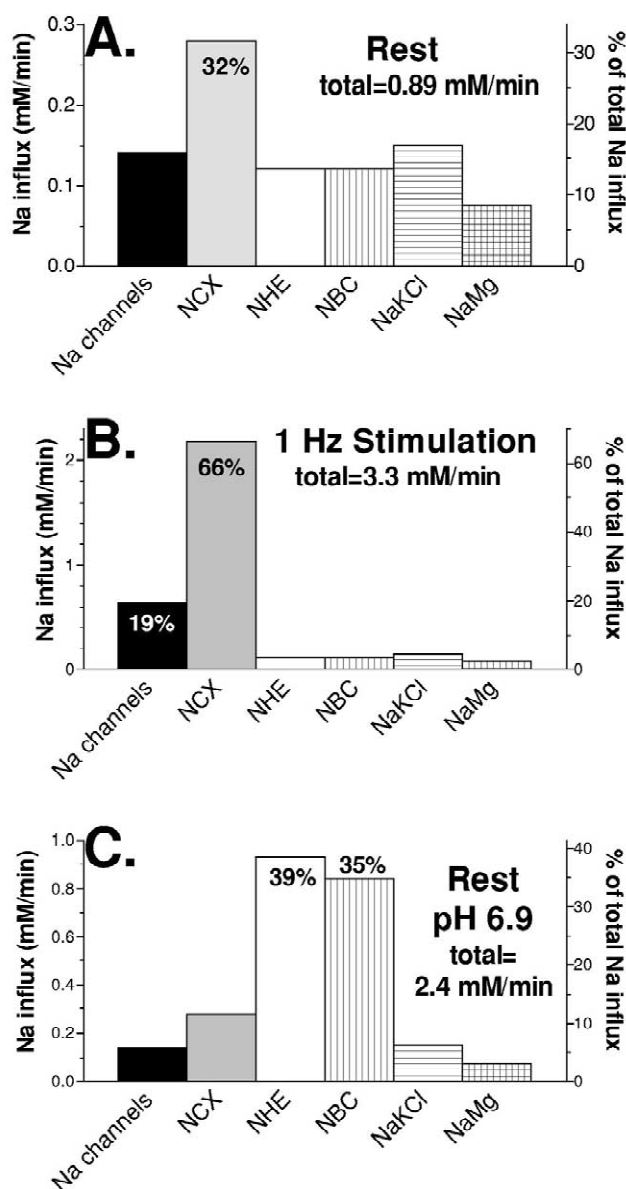


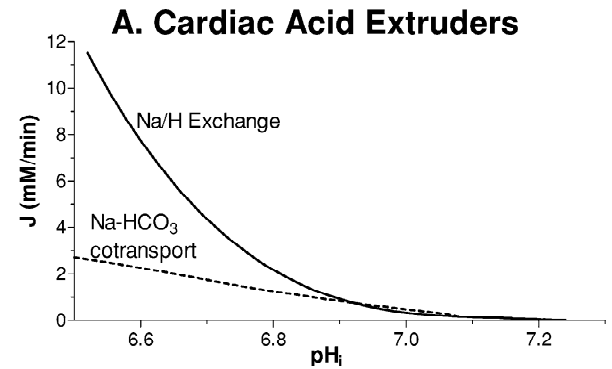
Fig. 4. The rate of  $\text{Na}^+$  influx in rabbit ventricular myocytes via different pathways at rest (A), during steady-state stimulation at 1 Hz (B, where only  $\text{Na}^+$  current and NCX were increased whereas the values measured in resting myocytes were used for all the other pathways) and in conditions of mild acidosis (C, where only NHE and NBC were increased according to Fig. 5A).



regulation of  $pH_i$  and cell volume. NHE functions mainly as a proton extruder in a 1  $Na^+$ :1  $H^+$  stoichiometry rendering the process electroneutral. There are at least six NHE isoforms thus far identified, with the NHE1–NHE5 apparently restricted to the plasma membrane whereas NHE6 might be the mitochondrial isoform [74] (but see Ref. [75]). NHE1, the so-called housekeeping isoform, is ubiquitously distributed in most tissues and is the primary NHE subtype found in mammalian cardiac cells [76,77]. NHE1 is a 110-kDa glycoprotein and consists of two principal domains: a 500-amino acid transmembrane domain and a 315-amino acid highly hydrophilic carboxyl-terminus cytoplasmic domain (for a review, see Ref. [76]). NHE1 contains 12 membrane-spanning regions that are critical for the maintenance of NHE1 function in terms of proton extrusion. The hydrophilic cytoplasmic region plays an important role in modulation of the exchanger, especially through phosphorylation-dependent reactions [78].

It has recently been suggested that NHE1 is localized primarily in the intercalated disk region of atrial and ventricular myocytes in close proximity to connexin 43, and, to a lesser degree, at the transverse tubular systems [79]. Such NHE1 localization could make NHE especially important in modulating cell-to-cell communication via gap junctions, and local signaling in T-tubules (although there is little functional data in this regard).

NHE activity is extremely sensitive to  $pH_i$ . The exchanger is allosterically activated by cytosolic protons, a drop in  $pH_i$  below a threshold level promoting the rapid extrusion of acid. Fig. 5A shows the  $pH_i$ -dependence of the rate of ion fluxes ( $Na^+$  influx,  $H^+$  efflux) through NHE in guinea-pig ventricular myocytes [80]. NHE is nearly inactive at a physiological  $pH_i$  of  $\sim 7.2$ , but it activates quickly when  $pH_i$  decreases. NHE activity in the heart seems to be species dependent, with a higher activity (determined as the rate of acid efflux at  $pH_i$  6.9) in rat (2.8 mM/min) versus human (1.1 mM/min) or guinea-pig (0.93 mM/min) ventricular myocytes [80,81]. We also found that at physiological  $pH_i$  (and 23 °C) the rate of  $Na^+$  entry via NHE is higher in rat (0.43 mM/min) versus rabbit (0.12 mM/min) ventricle [5]. Although intracellular  $Na^+$  can also affect NHE, it is unlikely to be a major regulator within a physiological range (4–16 mM) of  $[Na^+]_i$  [82]. Proton extrusion through NHE is also inhibited by extracellular acidosis [82]. This may be partly a thermodynamic effect (i.e. reducing the  $[H^+]$  gradient for proton extrusion), it may also be due to a competition of  $H^+$  with  $Na^+$  for binding to the external transport site of the exchanger [82]. The inhibition of NHE by extracellular acidosis may limit proton extrusion during ischemia, and relief of this inhibition upon reperfusion may contribute to a rapid activation of proton extrusion and  $Na^+$  entry [83]. A consequent gain in  $[Na^+]_i$  during reperfusion could also contribute to  $Ca^{2+}$  overload, diastolic dysfunction and arrhythmogenesis (due to NCX function). This may be why the NHE inhibitor cariporide (Hoe-642) is a protec-



## B. Resting Na Influx: Rabbit vs Rat

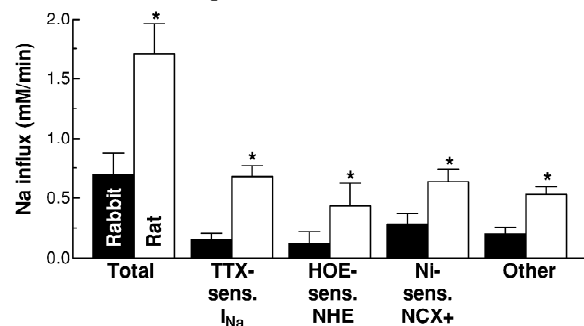


Fig. 5. (A) The  $pH_i$ -dependence of  $Na^+$  fluxes through cardiac NHE and NBC, as described in Ref. [80]. At physiological pH (7.0–7.2) the contribution of these transporters to  $Na^+$  influx is comparable (Fig. 2A). (B) The rate of  $Na^+$  influx through different pathways in resting rabbit and rat ventricular myocytes.  $Na^+$  influx was calculated as the initial slope of  $[Na^+]_i$  increase following abrupt  $Na^+/K^+$  pump inhibition [5]. TTX-, Hoe-642- and  $Ni^{2+}$ -sensitive  $Na^+$  influx was calculated as the difference between the total influx and the influx measured in the presence of 30  $\mu M$  TTX, 2  $\mu M$  Hoe-642, or 5 mM  $Ni^{2+}$ , respectively.

tive agent with respect to reperfusion injury [84,85]. While the events surrounding ischemia/reperfusion are complex and incompletely understood, it seems likely that NHE and NCX are importantly involved.

### 3.4. $Na^+/HCO_3^-$ cotransporter

$Na^+/HCO_3^-$  cotransport (NBC) also serves as an acid extruder in cardiac myocytes ( $Na^+$  and  $HCO_3^-$  influx). NBC was first described in the renal proximal tubule of the salamander [86], where it mediates  $Na^+$  and  $HCO_3^-$  efflux across the basolateral membrane. Functionally related cotransporters, which mediate both  $HCO_3^-$  influx and efflux, have now been described in many tissues, including the heart (reviewed in Ref. [87]). Cardiac NBC was originally suggested to have a stoichiometry ranging between 1:1 and 1:2 [88] and thus an equilibrium  $pH_i$  which, under most conditions, would favor acid extrusion. In guinea-pig ventricular myocytes [88] and sheep Purkinje fibers [89], acid extrusion via NBC appears to be voltage-insensitive, consistent with an electroneutral cotransporter.

Reports in cat papillary muscle [90] and rat ventricular myocytes [91] indicate a strong voltage-sensitivity, consistent with an electrogenic NBC, probably with a stoichiometry of  $1 \text{ Na}^+ : 2 \text{ HCO}_3^-$ . Two classes of electrogenic (NBCe [92] and NBC4 [93]) as well as one electroneutral [94] NBC carrier have been cloned and all three are present in the human heart at the mRNA level. However, the molecular identity of NBCs that mediate acid extrusion in heart cells from different species is not known. NBC is generally inhibited by stilbenes (DIDS and SITS), although the electroneutral isoform NBCn1 cloned from rat aorta is only very weakly inhibited by DIDS [95].

Leem et al. [80] measured the  $\text{pH}_i$ -dependence of NBC activity in guinea-pig ventricular myocytes and found that NBC activates roughly linearly with decreasing  $\text{pH}_i$ . Whether or not allosteric stimulation is involved is not known. Fig. 5 shows the  $\text{pH}_i$ -dependence of  $\text{Na}^+$  influx via NBC using the data from Ref. [80] and assuming a 1:1 stoichiometry of the cotransport (as reported for guinea-pig ventricular myocytes). It is notable that for relatively modest acid loads (i.e. to  $\text{pH}_i$  6.9), both NHE and NBC are stimulated about equally. Thus, at  $\text{pH}_i$  values within the normal physiological range, both transporters are about equally important for mediating acid extrusion and they contribute equally to  $\text{Na}^+$  influx. For larger intracellular acid challenges, NHE removes more acid than does NBC.

### 3.5. Other $\text{Na}^+$ influx pathways

#### 3.5.1. $\text{Na}^+/\text{K}^+/\text{2Cl}^-$ cotransporter

The  $\text{Na}^+/\text{K}^+/\text{2Cl}^-$  cotransporter (NKCC) was first detected in Ehrlich ascites tumor cells [96]. Since then, the cotransporter has been found in a variety of tissues, including the heart [97–99]. Two NKCC isoforms have been cloned: NKCC1, found in the membrane of a variety of cell types, and NKCC2, identified thus far only in the medullary regions of the kidney [99]. NKCC is inhibited by loop diuretics, such as furosemide and bumetanide. In all tissues investigated,  $\text{Na}^+/\text{K}^+/\text{2Cl}^-$  cotransport is electroneutral, with a stoichiometry of 1:1:2 and with an absolute requirement that  $\text{Na}^+$ ,  $\text{K}^+$  and  $\text{Cl}^-$  are all present on the same side of the membrane. In chick cardiac cells, the  $[\text{Cl}^-]$  and  $[\text{Na}^+]$  for half-maximal stimulation of the cotransporter are 59 and 40 mM, respectively [97]. Net transport may occur into or out of the cells, the magnitude and direction of this transport being determined by the sum of the chemical potential gradients of the transported ions. In physiological conditions,  $\text{Na}^+/\text{K}^+/\text{2Cl}^-$  cotransport is inwardly directed and thus maintains the intracellular  $[\text{Cl}^-]$  ( $[\text{Cl}^-]_i$ ) above its electrochemical equilibrium ( $\sim 15 \text{ mM}$ ). Intracellular  $\text{Cl}^-$  is an important regulator of the cotransporter, where high  $[\text{Cl}^-]_i$  inhibits ion fluxes in both directions. Gillen and Forbush [100] found a very steep relationship between bumetanide-sensitive ion flux and  $[\text{Cl}^-]_i$  in HEK-293 cells transfected with human NKCC1. In chick cardiac cells, the  $\text{Na}^+/\text{K}^+/\text{2Cl}^-$  cotransporter

accounts for 17% of the resting  $\text{Na}^+$  influx [97].  $\text{Na}^+/\text{K}^+/\text{2Cl}^-$  cotransport may be important in cell volume regulation [101].

#### 3.5.2. $\text{Na}^+/\text{Mg}^{2+}$ antiporter

The concentration of free  $\text{Mg}^{2+}$  in the cytoplasm ( $[\text{Mg}^{2+}]_i$ , 0.5–1 mM) is several hundred times lower than expected if  $\text{Mg}^{2+}$  ions were at electrochemical equilibrium. Since  $\text{Mg}^{2+}$  is a permeant ion across the plasmalemma, it must be constantly extruded from the cells. The main mechanism that removes  $\text{Mg}^{2+}$  from the cells is the  $\text{Na}^+/\text{Mg}^{2+}$  antiporter. However, its presence in the heart is controversial. Some studies reported the functional presence of  $\text{Na}^+/\text{Mg}^{2+}$  exchange in guinea-pig and ferret ventricle [102] whereas others found no evidence for it in guinea-pig [103] and chicken heart [104]. Such studies are generally based on changes in  $[\text{Mg}^{2+}]_i$  when  $[\text{Na}^+]_o$  is varied. However,  $\text{Mg}^{2+}$  is heavily buffered in cells and its membrane permeability is rather low, therefore the changes in  $[\text{Mg}^{2+}]_i$  are minimal. Also, changes in  $[\text{Na}^+]_o$  affect  $[\text{Ca}^{2+}]_i$  and  $\text{pH}_i$  and these in turn will affect intracellular  $\text{Mg}^{2+}$  buffering. Thus, the changes in  $[\text{Mg}^{2+}]_i$  in such protocols might not be mediated solely by the  $\text{Na}^+/\text{Mg}^{2+}$  exchanger. Tashiro and Konishi [105] used rat ventricular myocytes rendered  $\text{Mg}^{2+}$ -permeable with ionomycin in high  $[\text{Mg}^{2+}]_o$  conditions to facilitate passive  $\text{Mg}^{2+}$  influx. The rate of  $[\text{Mg}^{2+}]_i$  rise was significantly smaller in the presence of 140 mM external  $\text{Na}^+$  than in its absence. Washout of ionomycin and lowering extracellular  $\text{Mg}^{2+}$  caused rapid decline of  $[\text{Mg}^{2+}]_i$  when  $[\text{Na}^+]_o$  is 140 mM. This  $\text{Mg}^{2+}$  efflux was completely inhibited by withdrawal of extracellular  $\text{Na}^+$  and was largely attenuated by imipramine, a known inhibitor of  $\text{Na}^+/\text{Mg}^{2+}$  exchange. At 140 mM external  $\text{Na}^+$ , the rate of  $\text{Mg}^{2+}$  transport through the exchanger was 25–50  $\mu\text{M}/\text{min}$ .  $\text{Mg}^{2+}$  transport depended on  $[\text{Na}^+]_o$  according to a Hill-type curve, with the mid-point at  $\sim 80 \text{ mM}$  and a Hill coefficient of 2. This suggests that the exchanger has a stoichiometry of 2  $\text{Na}^+ : 1 \text{ Mg}^{2+}$  and therefore is electroneutral. A more complicated stoichiometry (2  $\text{Na}^+ + 2 \text{ K}^+ + 2 \text{ Cl}^- : 1 \text{ Mg}^{2+}$ ) has been proposed for the exchanger in squid giant axons and barnacle muscle cells [106].

There may also be other  $\text{Na}^+$  flux pathways that we have not discussed (e.g. background  $\text{Na}^+$  channels), but we feel that these are likely to be minor quantitatively. We can account for most of the measured  $\text{Na}^+$  fluxes by the mechanisms mentioned above (Fig. 4).

## 4. Balance of $\text{Na}^+$ influx and efflux

### 4.1. Quiescence

At steady state,  $\text{Na}^+$  influx and efflux must be equal. Fig. 4A shows the rate of resting  $\text{Na}^+$  influx through the

pathways discussed above. The values are based in part on our measurements in rabbit ventricular myocytes [5] and some extrapolations from guinea-pig data [80,102] and correspond to mammalian species with lower resting  $[Na^+]_i$  (i.e. other than rat and mouse). Adding the contribution of each pathway, the total  $Na^+$  influx in resting myocytes is 0.88 mM/min.  $Na^+$  influx pathways unaccounted for in Fig. 4A might increase this rate by ~0.1 mM/min [5]. Fig. 2A indicates that the  $Na^+/K^+$  pump will extrude this amount of  $Na^+$  if resting  $[Na^+]_i$  is 5.3 mM (5.5 mM if the additional 0.1-mM/min  $Na^+$  influx is considered). So, this principle of flux balance is also met with these quantitative resting  $Na^+$  flux estimates.

#### 4.2. Why is resting $[Na^+]_i$ higher in rat versus rabbit?

Now we can revisit the question of why resting  $[Na^+]_i$  in rat is higher than in rabbit ventricular myocytes. In reference to Fig. 2A we concluded that resting  $Na^+/K^+$ -ATPase-mediated  $Na^+$  efflux was higher in rat than rabbit and we inferred that this must be matched by higher  $Na^+$  influx. We evaluated resting  $Na^+$  influx by abrupt  $Na^+/K^+$ -ATPase block and measurement of the initial rate of rise of  $[Na^+]_i$  [5]. Indeed, as Fig. 5B shows, we found the resting  $Na^+$  influx to be 2.4 times higher in rat versus rabbit ventricular myocytes. Several  $Na^+$  influx pathways appear to contribute to different extents. For example, TTX-sensitive  $Na^+$  influx was almost five times higher in rat, while the Ni-sensitive  $Na^+$  influx (presumably mainly NCX) was only about two times higher in rat. These results confirm that the likely reason  $[Na^+]_i$  is higher in rat is because resting  $Na^+$  influx is higher. This would stimulate higher  $Na^+/K^+$ -ATPase-mediated  $Na^+$  efflux (and possibly  $Na^+/K^+$ -ATPase expression) until a new steady state balance is achieved at higher levels of both  $Na^+$  influx and efflux. This scenario might also hold for other species where  $[Na^+]_i$  is high (where mouse is like rat) and where  $[Na^+]_i$  is low (where guinea-pig is like rabbit).

#### 4.3. Stimulation

As described above  $Na^+$  influx is increased in contracting myocytes, at least because of increased  $Na^+$  entry via  $I_{Na}$  and NCX (Fig. 3). Fig. 4B shows estimates of  $Na^+$  influx in myocytes contracting at 1 Hz. The total  $Na^+$  influx in contracting cells is increased by ~3.7-fold (vs. rest) to ~3.5 mM/min. We only increased  $I_{Na}$  and NCX (by ~3 and 7-fold as discussed above), but certainly cannot exclude the possibility of increased  $Na^+$  influx by other pathways (e.g. NHE and NBC). This higher  $Na^+$  influx would require a matching increase in  $Na^+$  efflux via the  $Na^+/K^+$  pump and this would occur at ~11 mM  $[Na^+]_i$  (Fig. 2A). This is higher than the  $[Na^+]_i$  we measure in rabbit at 1-Hz stimulation (~8 mM). Part of this difference could reflect restricted subsarcolemmal diffusion of  $Na^+$

(see below). It will be valuable for additional quantitative data to be measured for these estimates to be further refined. In conclusion, while the various  $Na^+$  influx pathways differ little at rest with only NCX being much larger than the others (and only by ~2-fold),  $Na^+$  channels and NCX are likely to become much more dominant during normal electrical and contractile activity (in this example providing 85% of the total  $Na^+$  influx).

#### 4.4. Acidosis

Acidosis is a major consequence of myocardial ischemia and contributes to the ischemic decline in force. The major negative inotropic effect is mainly due to intracellular versus extracellular acidosis and is caused in large part by decreased myofilament  $Ca^{2+}$  sensitivity.  $Ca^{2+}$  transient amplitude during abrupt acidosis can be initially increased, unchanged or decreased [107–109]. However, in almost all reports there is then a progressive increase in twitch  $\Delta[Ca^{2+}]_i$  and this causes a partial recovery of contractions. Acidosis can also gradually increase diastolic  $[Ca^{2+}]_i$  [110].

Low  $pH_i$  stimulates proton extrusion via NHE and NBC (Fig. 5A), especially when  $pH_o$  is relatively normal. Thus, resting  $Na^+$  influx is enhanced during acidosis. Fig. 4C shows estimations of the rate of resting  $Na^+$  influx through various pathways in the case of a mild acidosis ( $pH_i$  6.9). With respect to Fig. 4A only NHE and NBC were increased as predicted from Fig. 5A. Of course there may also be inhibition of other  $Na^+$  influx pathways as well (e.g. NCX and  $I_{Na}$ ). Our expectation is that NHE and NBC increase greatly and in this case account for 75% of resting  $Na^+$  influx. Furthermore, the  $Na^+/K^+$  pump is partially inhibited at low  $pH_i$  [111]. These two factors lead to an increase in  $[Na^+]_i$  [112], which may contribute to the slow recovery of contractility via a shift in NCX and increase in  $[Ca^{2+}]_i$ . NCX is also inhibited by low  $pH_i$  [113]. This may limit the ability of NCX to extrude  $Ca^{2+}$  (especially at high  $[Na^+]_i$ ). As with cardiac glycosides, this may also contribute to increased SR  $Ca^{2+}$  content and larger  $Ca^{2+}$  transients seen during acidosis, but could also lead to  $Ca^{2+}$  overload and consequent arrhythmias.

During severe hypoxia (associated with ischemia) there is a large rise in  $[Na^+]_i$  which can reach 40 mM in prolonged anoxia. Eigel and Hadley [114] evaluated the cellular basis of the  $Na^+$  gain. The main mechanisms of net  $Na^+$  gain during anoxia were TTX sensitive  $Na^+$  channels and Hoe-642-sensitive  $Na^+/H^+$  exchange. TTX and Hoe-642 each blocked ~50% of the  $Na^+$  gain during simple anoxia. For anoxia plus extracellular acidosis the  $Na^+$  gain was blocked by TTX, but not by Hoe-642. However, when anoxia or acidosis (pH 6.85) was coupled with high  $[K^+]_o$  (10 mM) to simulate ischemia, the  $Na^+$  gain was suppressed almost completely by Hoe-642, but not by TTX. It is unclear why  $Na^+$  channel influx would

occur in the cases with normal  $[K^+]_o$  (while cells are quiescent), but anoxia and ischemic metabolites have been shown to produce persistent  $Na^+$  channel opening in ventricular myocytes [115,116]. Since depolarization prevented the TTX-sensitive  $Na^+$  gain, it is possible that anoxia allows a tiny window  $I_{Na}$  at resting  $E_m$ , but inactivation prevails upon depolarization in high  $[K^+]_o$ . Thus, during ischemia  $[Na^+]_i$  rise may be mediated by  $Na^+/H^+$  exchange and  $Na^+$  channel entry [117].

## 5. Mitochondrial $Na^+$ transport

Fig. 1B shows mitochondrial  $Na^+$  movements.  $[Na^+]_i$  can importantly regulate mitochondrial  $[Ca^{2+}]$ , because mitochondrial  $Ca^{2+}$  extrusion occurs mainly via a  $Na^+/Ca^{2+}$  antiporter, which may be electroneutral ( $2 Na^+:1 Ca^{2+}$ ), but might also be  $>2:1$  [118–120]. The  $[Na^+]_i$  dependence of this  $Na^+/Ca^{2+}$  antiporter is sigmoidal with half-maximal activity at  $\sim 5$ – $8$  mM  $Na^+$ , making this system sensitive to physiological  $[Na^+]_i$  changes [118,121]. While variations in bulk cytoplasmic  $[Na^+]$  during the cardiac cycle are probably insufficient to cause rapid release of mitochondrial  $Ca^{2+}$ , large changes in  $[Na^+]$  can induce substantial mitochondrial  $Ca^{2+}$  release in vitro [118]. The  $V_{max}$  value for  $Ca^{2+}$  extrusion (and  $Na^+$  entry) via mitochondrial  $Na^+/Ca^{2+}$  exchange in the heart is  $\sim 15$  nmol  $Ca/mg$  protein per min [122] or  $\sim 0.9$  mM/min. This gives the mitochondrial  $Na^+/Ca^{2+}$  antiport comparable flux capacity to some sarcolemmal  $Na^+$  transporters.

$Na^+$  entering mitochondria through the  $Na^+/Ca^{2+}$  antiporter is then extruded via a  $Na^+/H^+$  exchange system, driven by the electrochemical gradient of protons (which is created by the electron transport chain). The mitochondrial  $Na^+/H^+$  exchanger is reversible and seems to be symmetrical in its interaction with  $Na^+$  [123]. The  $K_m$  for  $Na^+$  transport is  $\sim 26$  mM at an intramitochondrial pH of 8.0 [124] and decreases with more alkaline mitochondrial pH. Matrix protons compete with  $Na^+$  for binding to a common site and thus inhibit the exchanger with a mid-point of  $\sim 30$  nM (pH  $\sim 7.5$ ) [125]. The mitochondrial  $Na^+/H^+$  antiport shares many properties with the sarcolemmal NHE, however it differs in some aspects such as the sensitivity to amiloride analogues and relative lack of regulation [123].

Mitochondrial  $[Na^+]$  ( $[Na^+]_m$ ) appears to be lower than  $[Na^+]_i$  [8,126].  $[Na^+]_m$  increases linearly with  $[Na^+]_i$  and the  $[Na^+]$  gradient across the mitochondrial inner membrane depends on the energetic state of the mitochondria [126]. In isolated mitochondria, the  $Na^+$  gradient was equal to the electrochemical  $H^+$  gradient over a wide range of external  $[Na^+]$  and changed rapidly in response to changes in matrix pH [126], suggesting that  $Na^+$  distribution across the inner mitochondrial membrane is effectively determined by the equilibrium of the  $Na^+/H^+$  antiporter. The quantitative role of mitochondria in overall

$[Na^+]_i$  regulation is unclear. While in heart, mitochondria occupy  $\sim 35\%$  of the total cell volume it should be kept in mind that mitochondria are a totally intracellular compartment and as such are a limited source or sink. However, since  $[Na^+]_m$  rises with  $[Na^+]_i$ ,  $Na^+$  entry into mitochondria may serve as a buffer for  $[Na^+]_i$ , and could limit changes in  $[Na^+]_i$  during pathophysiological conditions.

## 6. Intracellular $Na^+$ gradients

Several studies have provided evidence for the presence of a  $[Na^+]$  gradient between the subsarcolemmal space ( $[Na^+]_{sm}$ ) and bulk cytosol in arterial smooth muscle [127] and cardiac myocytes [128–132]. The existence of such intracellular  $[Na^+]$  gradients implies restricted diffusion with respect to transport rate. Wendt-Gallitelli et al. [133] used electron probe microanalysis to measure  $[Na^+]$  in a volume within 20 nm of the inner side of the sarcolemma of guinea-pig ventricular myocytes.  $[Na^+]_{sm}$  increased up to 40 mM during stimulation of the cells, with no change in bulk  $[Na^+]_i$ . This steep subsarcolemmal  $[Na^+]$  gradient dissipated, but only within minutes of the end of stimulation. This is surprisingly slow dissipation of such a  $[Na^+]$  gradient, and this method measures total rather than free  $[Na^+]$ . This could reflect increased binding of  $Na^+$  in a subsarcolemmal space, which could in turn alter  $Na^+$  diffusion.

A transient peak in the  $Na^+/K^+$  pump current has been observed in voltage-clamped ventricular myocytes, when the  $Na^+/K^+$  pump was abruptly reactivated after a period of pump blockade [1,128,131].  $I_{pump}$  then decayed over a few minutes to a steady-state level. This  $I_{pump}$  sag might be the result of lowering  $[Na^+]_{sm}$  because of the pump activity (even when global  $[Na^+]_i$  was presumed or measured to be little changed). Peak  $I_{pump}$  also increased in response to a train of depolarizations prior to  $Na^+/K^+$  pump reactivation [134], suggesting that activation of  $Na^+$  channels increases  $[Na^+]_{sm}$ . Lipp and Niggli [135] have also observed that  $I_{Na}$  can activate  $Ca^{2+}$  influx via NCX, inferring that  $I_{Na}$  raised  $[Na^+]_{sm}$ . While some preliminary data imply that  $I_{Na}$  may not modify local  $[Na^+]_{sm}$  sufficiently to alter NCX or  $Na^+/K^+$ -ATPase [136,137], the whole issue of  $[Na^+]_i$  gradients requires further study.

Su et al. [134] showed that abrupt  $Na^+/K^+$ -ATPase inhibition in mouse ventricular myocytes increases the efficacy of a given  $I_{Ca}$  to trigger SR  $Ca^{2+}$  release (Fig. 6). This was interpreted as a prevention of  $Na^+$  extrusion in the SR junctional cleft allowing local cleft  $[Na^+]_{sm}$  to rise and favor  $Ca^{2+}$  entry via NCX. Abrupt  $Na^+/K^+$  pump inhibition was also shown to slow the decline of caffeine-induced  $Ca^{2+}$  transients and  $I_{NCX}$  [132]. Goldhaber et al. [138] also found that abrupt removal of  $[Na^+]_o$  caused an increase in resting  $Ca^{2+}$  spark frequency, and they attributed this to a blockade of tonic  $Ca^{2+}$  removal from the junctional cleft by  $Na^+/Ca^{2+}$  exchange. All of these data

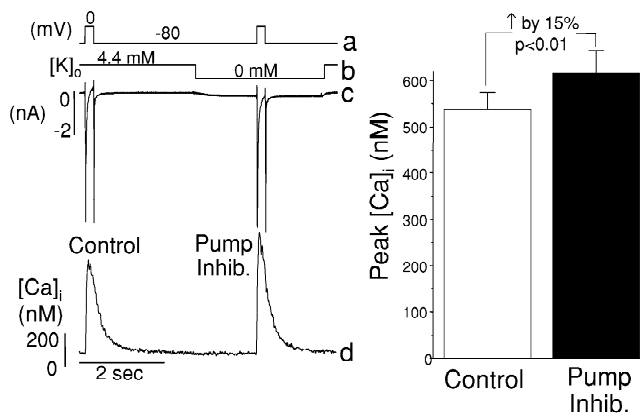


Fig. 6. Effects of abrupt inhibition of the  $\text{Na}^+/\text{K}^+$  pump (Pump Inhib.) on  $[\text{Ca}^{2+}]_i$  transients and membrane currents. The left panel shows the last of a series of eight voltage-clamp steps ( $-80$  to  $0$  mV) to induce a stable  $[\text{Ca}^{2+}]_i$  transient magnitude (a), membrane currents (c, including  $I_{\text{Na}}$  and  $I_{\text{Ca}}$ ) and  $[\text{Ca}^{2+}]_i$  transients (d). Abrupt Pump Inhib. (by  $[\text{K}^+]_o$  removal using a rapid solution switcher, b) for  $1.5$  s immediately before and during the test pulse was evidenced by the inward shift in holding current (c). With Pump Inhib. peak  $[\text{Ca}^{2+}]_i$  was significantly higher (d and bar graph). Results are mean  $\pm$  S.E.M. of 16 cells. Pipette  $[\text{Na}^+]$  was  $15$  mM. (From Su et al. [134])

suggest that local or junctional microdomain  $[\text{Na}^+]_{\text{sm}}$  and  $[\text{Ca}^{2+}]_i$  may be controlled by local  $\text{Na}^+/\text{K}^+$ -ATPase,  $\text{Na}^+$  channels and NCX, such that, when the system is not at steady-state, they differ significantly from bulk  $[\text{Na}^+]_i$  and  $[\text{Ca}^{2+}]_i$ . Thus, a normally functioning  $\text{Na}^+/\text{K}^+$ -ATPase may maintain  $[\text{Na}^+]_i$  and  $[\text{Ca}^{2+}]_i$  in the junctional cleft at lower values than bulk cytosolic, and this may limit CICR. These issues, however, merit further study and quantitative characterization. Some of these results are difficult to reconcile with expected ion diffusional characteristics in cells or are counterbalanced by other results. For example, ultrastructural studies also indicate that  $\text{Na}^+$  channels, NCX and SR  $\text{Ca}^{2+}$  release channels in rat ventricular myocytes are not co-localized with each other [139]. On the other hand, the  $\text{Na}^+/\text{K}^+$  pump and NCX are co-localized in smooth muscle [140]. It appears that there is much still to learn about cellular  $\text{Na}^+$  regulation. We hope that this integrative overview of cardiac  $\text{Na}^+$  regulation helps to provide an initial semi-quantitative framework for future work and subsequent articles in this focused issue.

## Acknowledgements

This work was supported by NIH grants HL64098 and HL64724 (D.M.B.) and HL53773 (W.H.B.).

## References

[1] Despa S, Bers DM. Simultaneous measurements of  $[\text{Na}]_i$  and  $\text{Na}/\text{K}$  pump current in rabbit ventricular myocytes. *Biophys J* 2002;82:68, (abstract).

[2] Gray RP, McIntyre H, Sheridan DS, Fry CH. Intracellular sodium and contractile function in hypertrophied human and guinea-pig myocardium. *Pflügers Arch* 2001;442:117–123.

[3] Yao A, Su Z, Nonaka A et al. Abnormal myocyte  $\text{Ca}^{2+}$  homeostasis in rabbits with pacing-induced heart failure. *Am J Physiol* 1998;275:H1441–H1448.

[4] Harrison SM, McCall E, Boyet MR. The relationship between contraction and intracellular sodium in rat and guinea-pig ventricular myocytes. *J Physiol* 1992;449:517–550.

[5] Despa S, Islam MA, Pogwizd SM, Bers DM. Intracellular  $[\text{Na}^+]_i$  and  $\text{Na}^+$ -pump rate in rat and rabbit ventricular myocytes. *J Physiol* 2002;539:133–143.

[6] Levi AJ, Lee CO, Brooksby P. Properties of the fluorescent sodium indicator SBFI in rat and rabbit cardiac myocytes. *J Cardiovasc Electrophysiol* 1994;5:241–257.

[7] Shattock MJ, Bers DM. Rat versus rabbit ventricle:  $\text{Ca}$  flux and intracellular  $\text{Na}$  assessed by ion-selective microelectrodes. *Am J Physiol* 1989;256:C813–C822.

[8] Donoso P, Mill JG, O'Neil SC, Eisner DA. Fluorescence measurements of cytoplasmic and mitochondrial sodium concentration in rat ventricular myocytes. *J Physiol* 1992;448:493–509.

[9] Yao AS, Su Z, Nonaka A et al. Effects of overexpression of the  $\text{Na}^+-\text{Ca}^{2+}$  exchanger on  $[\text{Ca}^{2+}]_i$  transients in murine ventricular myocytes. *Circ Res* 1998;82:657–665.

[10] Cook SJ, Chamunorwa JP, Lancaster MK, O'Neill SC. Regional differences in the regulation of intracellular sodium and in action potential configuration in rabbit left ventricle. *Pflügers Arch* 1997;433:515–522.

[11] Lancaster MK, Bennet DL, Cook SJ, O'Neill SC.  $\text{Na}/\text{K}$  pump  $\alpha$  subunit expression in rabbit ventricle and regional variations of intracellular  $\text{Na}$  regulation. *Pflügers Arch* 2000;440:735–739.

[12] Bers DM. Excitation-contraction coupling and cardiac contractile force. Dordrecht, The Netherlands: Kluwer, 2001.

[13] Lee CO, Dagostino M. Effect of strophanthidin on intracellular  $\text{Na}$  ion activity and twitch tension on constantly driven canine cardiac Purkinje fibers. *Biophys J* 1982;40:185–198.

[14] Harrison SM, Bers DM. The influence of temperature on the calcium sensitivity of the myofilaments of skinned ventricular muscle from the rabbit. *J Gen Physiol* 1989;93:411–427.

[15] Lauger P. Electrogenic ion pumps. Sunderland, Massachusetts: Sinauer Associates, Inc, 1991.

[16] Blanco G, Mercer RW. Isozymes of the  $\text{Na}-\text{K}-\text{ATPase}$ : heterogeneity in structure, diversity in function. *Am J Physiol* 1998;275:F633–F650.

[17] Shull GE, Schwartz A, Lingrel JB. Amino-acid sequence of the catalytic subunit of the  $(\text{Na}^+,\text{K}^+)-\text{ATPase}$  deduced from a complementary DNA. *Nature* 1985;316:691–695.

[18] Kawakami K, Noguchi S, Noda M et al. Primary structure of the  $\alpha$ -subunit of *Torpedo californica*  $(\text{Na}^+,\text{K}^+)-\text{ATPase}$  deduced from cDNA sequence. *Nature* 1985;316:733–736.

[19] Mercer RW, Biemesderfer D, Bliss DP, Collins JH, Forbush B. Molecular cloning and immunological characterization of the  $\gamma$ -polypeptide, a small protein associated with the  $\text{Na},\text{K}-\text{ATPase}$ . *J Cell Biol* 1993;121:579–586.

[20] Shamraj OI, Lingrel JB. A putative fourth  $\text{Na}^+,\text{K}^+ -\text{ATPase}$   $\alpha$  subunit gene is expressed in testis. *Proc Natl Acad Sci USA* 1994;91:12952–12956.

[21] Zahler R, Gilmore-Hebert M, Baldwin JC, Franco K, Benz Jr. EJ. Expression of  $\alpha$  isoforms of the  $\text{Na},\text{K}-\text{ATPase}$  in human heart. *Biochim Biophys Acta* 1993;1149:1890194.

[22] Wang J, Schwinger RH, Frank K et al. Regional expression of sodium pump subunit isoforms and  $\text{Na}^+-\text{Ca}^{2+}$  exchanger in the human heart. *J Clin Invest* 1996;98:1650–1658.

[23] McDonough AA, Zhang Y, Shin V, Frank JS. Subcellular distribution of  $\text{Na}$  pump isoform subunits in mammalian cardiac myocytes. *Am J Physiol* 1996;270:C1221–C1227.

[24] Kim CH, Fan TH, Kelly PF et al. Isoform-specific regulation of myocardial  $\text{Na},\text{K}-\text{ATPase}$   $\alpha$ -subunit in congestive heart failure. Role of norepinephrine. *Circulation* 1994;89:313–320.

- [25] Zahler R, Gilmore-Hebert M, Sun W, Benz Jr. EJ. Na,K-ATPase isoform gene expression in normal and hypertrophied dog heart. *Basic Res Cardiol* 1996;91:256–266.
- [26] Ng YC, Book CB. Expression of Na<sup>+</sup>-K<sup>+</sup>-ATPase  $\alpha$ 1 and  $\alpha$ 3-isoforms in adult and neonatal ferret hearts. *Am J Physiol* 1992;263:H1430–H1436.
- [27] Baba A, Yoshikawa T, Nakamura I, Iwata M, Wainai Y, Ogawa S. Isoform-specific alterations in cardiac and erythrocyte Na<sup>+</sup>,K<sup>+</sup>-ATPase activity induced by norepinephrine. *J Card Fail* 1998;4:333–341.
- [28] Gao J, Wymore R, Wymore RT et al. Isoform-specific regulation of the sodium pump by  $\alpha$ - and  $\beta$ -adrenergic agonists in the guinea-pig ventricle. *J Physiol* 1999;516:377–383.
- [29] Orlowski J, Lingrel JB. Tissue specific and developmental regulation of rat Na,K-ATPase catalytic  $\alpha$  isoform and  $\beta$  subunit mRNAs. *J Biol Chem* 1988;263:10436–10442.
- [30] Lucchesi PA, Sweadner KJ. Postnatal changes in Na,K-ATPase isoform expression in rat cardiac ventricle. *J Biol Chem* 1991;266:9327–9331.
- [31] Charlemagne D, Orlowski J, Oliviero P et al. Alteration of Na,K-ATPase subunit mRNA and protein levels in hypertrophied rat heart. *J Biol Chem* 1994;269:1541–1547.
- [32] Semb SO, Lunde PK, Holt E, Tonnessen T, Christensen G, Sejersted OM. Reduced myocardial Na-K pump capacity in congestive heart failure following myocardial infarction in rats. *J Mol Cell Cardiol* 1998;30:1311–1328.
- [33] Pierre S, Paganelli F, Sennoune S et al. RT-PCR detection of the Na,K-ATPase  $\beta$ <sub>3</sub>-isoform in human heart. *Cell Mol Biol (Noisy-le-grand)* 2001;47:261–264.
- [34] Wang J, Velotta JB, McDonough AA, Farley RA. All human Na<sup>+</sup>-K<sup>+</sup>-ATPase  $\alpha$  subunit isoforms have a similar affinity for cardiac glycosides. *Am J Physiol* 2001;281:C1336–C1343.
- [35] James PF, Grupp IL, Grupp G et al. Identification of a specific role for the Na,K-ATPase  $\alpha$ 2 isoform as a regulator of calcium in the heart. *Mol Cell* 1999;3:555–563.
- [36] Juhaszova M, Blaustein MP. Na<sup>+</sup> pump low and high ouabain affinity  $\alpha$  subunit isoforms are differently distributed in cells. *Proc Natl Acad Sci USA* 1997;94:1800–1805.
- [37] Glitsch HG, Tappe A. Change of Na<sup>+</sup> pump current reversal potential in sheep cardiac Purkinje cells with varying free energy of ATP hydrolysis. *J Physiol* 1995;484:605–616.
- [38] Hilgemann DW, Nagel GA, Gadsby DC. Na/K pump current in giant membrane patches excised from ventricular myocytes. In: Kaplan JH, De Weer P, editors. *The sodium pump: recent developments*. New York: Rockefeller University Press, 1991, pp. 543–547.
- [39] Friedrich T, Bamberg E, Nagel G. Na<sup>+</sup>,K<sup>+</sup>-ATPase pump currents in giant excised patches activated by an ATP concentration jump. *Biophys J* 1996;71:2486–2500.
- [40] Glitsch HG, Tappe A. The Na<sup>+</sup>/K<sup>+</sup> pump of cardiac Purkinje cells is preferentially fuelled by glycolytic ATP production. *Pflügers Arch* 1993;422:380–385.
- [41] Glitsch HG. Electrophysiology of the sodium-potassium-ATPase in cardiac cells. *Physiol Rev* 2001;81:1791–1826.
- [42] Therien AG, Blostein R. K<sup>+</sup>/Na<sup>+</sup> antagonism at cytoplasmic sites of Na<sup>+</sup>-K<sup>+</sup>-ATPase: a tissue-specific mechanism of sodium pump regulation. *Am J Physiol* 1999;277:C891–C898.
- [43] Nakao M, Gadsby DC. [Na] and [K] dependence of the Na/K pump current-voltage relationship in guinea pig ventricular myocytes. *J Gen Physiol* 1989;94:539–565.
- [44] Gadsby DC, Kimura J, Noma A. Voltage dependence of Na/K pump current in isolated heart cells. *Nature* 1985;315:63–65.
- [45] Rakowski RF, Gadsby DC, De Weer P. Voltage dependence of the Na/K pump. *J Membr Biol* 1997;155:105–113.
- [46] Zahler R, Zhang Z-T, Manor M, Boron WF. Sodium kinetics of Na,K-ATPase  $\alpha$  isoforms in intact transfected HeLa cells. *J Gen Physiol* 1997;110:201–213.
- [47] Liu X, Songu-Mize E. Effect of Na on Na<sup>+</sup>,K<sup>+</sup>-ATPase  $\alpha$  subunit expression and Na pump activity. *Eur J Pharmacol* 1998;351:113–119.
- [48] Catterall WA. Cellular and molecular biology of voltage-gated Na channels. *Physiol Rev* 1992;72:S15–S48.
- [49] Stühmer W, Conti F, Suzuki H et al. Structural parts involved in activation and inactivation of the sodium channel. *Nature* 1989;339:597–603.
- [50] Isom LL, De Jongh KS, Catterall WA. Auxiliary subunits of voltage-gated ion channels. *Neuron* 1994;12:1183–1194.
- [51] Saint DA, Ju YK, Gage PW. A persistent sodium current in rat ventricular myocytes. *J Physiol* 1992;453:219–231.
- [52] Maltsev VA, Sabbah HN, Higgins RS, Silverman N, Lesch M, Undrovinas AI. Novel, ultraslow inactivating sodium current in human ventricular cardiomyocytes. *Circulation* 1998;98:2545–2552.
- [53] Undrovinas AI, Maltsev VA, Sabbah HN. Repolarization abnormalities in cardiomyocytes of dogs with chronic heart failure: role of sustained inward current. *Cell Mol Life Sci* 1999;55:494–505.
- [54] Satoh H, Delbridge LM, Blatter LA, Bers DM. Surface:volume relationship in cardiac myocytes studied with confocal microscopy and membrane capacitance measurements: species-dependence and developmental effects. *Biophys J* 1996;70:1494–1504.
- [55] Despa S, Islam MA, Pogwizd SM, Bers DM. Intracellular Na<sup>+</sup> concentration is elevated in heart failure, but Na/K-pump function is unchanged. *Circulation* 2002;105:2543–2548.
- [56] Blaustein MP, Lederer WJ. Sodium/calcium exchange: its physiological implications. *Physiol Rev* 1999;79:763–854.
- [57] Philipson KD, Nicoll DA. Sodium–calcium exchange: a molecular perspective. *Annu Rev Physiol* 2000;62:111–133.
- [58] Shigekawa M, Iwamoto T. Cardiac Na<sup>+</sup>–Ca<sup>2+</sup> exchange: molecular and pharmacological aspects. *Circ Res* 2001;88:864–876.
- [59] Matsuoka S, Nicoll DA, Reilly RF, Hilgemann DW, Philipson KD. Initial localization of regulatory regions of the cardiac sarcolemmal Na<sup>+</sup>–Ca<sup>2+</sup> exchanger. *Proc Natl Acad Sci USA* 1993;90:3870–3874.
- [60] Philipson KD, Nicoll DA. Molecular and kinetic aspects of sodium–calcium exchange. *Int Rev Cytol* 1993;137C:199–227.
- [61] Nicoll DA, Ottolia M, Lu L, Lu Y, Philipson KD. A new topological model of the cardiac sarcolemmal Na<sup>+</sup>–Ca<sup>2+</sup> exchanger. *J Biol Chem* 1999;274:910–917.
- [62] Hilgemann DW, Nicoll DA, Philipson KD. Charge movement during Na<sup>+</sup> translocation by native and cloned cardiac Na<sup>+</sup>/Ca<sup>2+</sup> exchanger. *Nature* 1991;352:715–718.
- [63] Fujioka Y, Komeda M, Matsuoka S. Stoichiometry of Na<sup>+</sup>–Ca<sup>2+</sup> exchange in inside-out patches excised from guinea-pig ventricular myocytes. *J Physiol* 2000;523:339–351.
- [64] Dong H, Dunn J, Lytton J. Stoichiometry of the cardiac Na<sup>+</sup>/Ca<sup>2+</sup> exchanger NCX1.1 measured in transfected HEK cells. *Biophys J* 2002;82:1943–1952.
- [65] Egger M, Niggli E. Paradoxical block of the Na<sup>+</sup>–Ca<sup>2+</sup> exchanger by extracellular protons in guinea-pig ventricular myocytes. *J Physiol* 2000;523:353–366.
- [66] Weber CR, Ginsburg KS, Philipson KD, Shannon TR, Bers DM. Allosteric regulation of Na/Ca exchange current by cytosolic Ca in intact cardiac myocytes. *J Gen Physiol* 2001;117:119–131.
- [67] Hilgemann DW, Matsuoka S, Nagel GA, Collins A. Steady-state and dynamic properties of cardiac sodium–calcium exchange. Sodium-dependent inactivation. *J Gen Physiol* 1992;100:905–932.
- [68] Diaz ME, Trafford AW, O'Neill SC, Eisner DA. Measurement of sarcoplasmic reticulum Ca<sup>2+</sup> content and sarcolemmal Ca<sup>2+</sup> fluxes in isolated rat ventricular myocytes during spontaneous Ca<sup>2+</sup> release. *J Physiol* 1997;501:3–16.
- [69] Trafford AW, Diaz ME, Negretti N, Eisner DA. Enhanced Ca<sup>2+</sup> current and decreased Ca<sup>2+</sup> efflux restore sarcoplasmic reticulum Ca<sup>2+</sup> content after depletion. *Circ Res* 1997;81:477–484.
- [70] Su Z, Bridge JHB, Philipson KD, Spitzer KW, Barry WH. Quantitation of Na/Ca exchanger function in single ventricular myocytes. *J Mol Cell Cardiol* 1999;31:1125–1135.

- [71] Choi HS, Trafford AW, Eisner DA. Measurement of calcium entry and exit in quiescent rat ventricular myocytes. *Pflügers Arch* 2000;440:600–608.
- [72] Satoh H, Blatter LA, Bers DM. Effects of  $[Ca]_i$ ,  $Ca^{2+}$  load and rest on  $Ca^{2+}$  spark frequency in ventricular myocytes. *Am J Physiol* 1997;272:H657–668.
- [73] Weber CR, Piacentino III V, Ginsburg KS, Houser SR, Bers DM.  $Na^+-Ca^{2+}$  exchange current and submembrane  $[Ca^{2+}]$  during the cardiac action potential. *Circ Res* 2002;90:182–189.
- [74] Numata M, Petrecca K, Lake N, Orlowski J. Identification of a mitochondrial  $Na^+/H^+$  exchanger. *J Biol Chem* 1998;273:6951–6959.
- [75] Brett CL, Wei Y, Donowitz M, Rao R. Human  $Na^+/H^+$  exchanger isoform 6 is found in recycling endosomes of cells, not in mitochondria. *Am J Physiol* 2002;282:C1031–1041.
- [76] Orlowski J, Grinstein S.  $Na^+/H^+$  exchangers of mammalian cells. *J Biol Chem* 1997;272:22373–22376.
- [77] Karmazyn M, Gan XT, Humphreys RA, Yoshida H, Kusumoto K. The myocardial  $Na^+-H^+$  exchange: structure, regulation, and its role in heart disease. *Circ Res* 1999;85:777–786.
- [78] Coumilion L, Pouyssegur J. Structure-function studies and molecular regulation of the growth factor activatable sodium–hydrogen exchanger (NHE-1). *Cardiovasc Res* 1995;29:147–154.
- [79] Petrecca K, Atanasiu R, Grinstein S, Orlowski J, Shrier A. Subcellular localization of the  $Na^+/H^+$  exchanger NHE1 in rat myocardium. *Am J Physiol* 1999;276:H709–H717.
- [80] Leem CH, Lagadic-Gossmann D, Vaughan-Jones RD. Characterization of intracellular pH regulation in the guinea-pig ventricular myocytes. *J Physiol* 1999;509:487–496.
- [81] Yokoyama H, Gunasegaram S, Harding SE, Avkiran M. Sarcolemmal  $Na^+/H^+$  exchanger activity and expression in human ventricular myocardium. *J Am Coll Cardiol* 2000;36:534–540.
- [82] Wu ML, Vaughan-Jones RD. Interaction between  $Na^+$  and  $H^+$  ions on  $Na-H$  exchange in sheep cardiac Purkinje fibers. *J Mol Cell Cardiol* 1997;29:1131–1140.
- [83] Lazdunski M, Frelin C, Vigne P. The sodium/hydrogen exchange system in cardiac cells: its biochemical and pharmacological properties and its role in regulating internal concentrations of sodium and internal pH. *J Mol Cell Cardiol* 1985;17:1029–1042.
- [84] Xue YX, Aye NN, Hashimoto K. Antiarrhythmic effects of HOE642, a novel  $Na^+-H^+$  exchanger inhibitor, on ventricular arrhythmias in animal hearts. *Eur J Pharmacol* 1996;317:309–316.
- [85] Stromer H, de Groot MC, Horn M et al.  $Na^+/H^+$  exchange inhibition with HOE642 improves postischemic recovery due to attenuation of  $Ca^{2+}$  overload and prolonged acidosis on reperfusion. *Circulation* 2000;101:2749–2755.
- [86] Boron WF, Boulpaep EL. Intracellular pH regulation in the renal proximal tubule of the salamander. *J Gen Physiol* 1983;8:53–94.
- [87] Romero MF, Boron WF. Electrogenic  $Na^+/HCO_3^-$  cotransporters: cloning and physiology. *Annu Rev Physiol* 1999;61:699–723.
- [88] Lagadic-Gossmann D, Buckler KJ, Vaughan-Jones RD. Role of bicarbonate in pH recovery from intracellular acidosis in the guinea-pig ventricular myocyte. *J Physiol* 1992;458:361–384.
- [89] Dart C, Vaughan-Jones RD.  $Na^+-HCO_3^-$  symport in the sheep cardiac Purkinje fibre. *J Physiol* 1992;451:365–385.
- [90] Camili6n de Hurtado MC, P6rez NG, Cingolani HE. An electrogenic sodium-bicarbonate cotransport in the regulation of myocardial intracellular pH. *J Mol Cell Cardiol* 1995;27:231–242.
- [91] Aiello EA, Vila Petroff MG, Mattiazzi AR, Cingolani HE. Evidence for an electrogenic  $Na^+-HCO_3^-$  symport in rat cardiac myocytes. *J Physiol* 1998;512:137–148.
- [92] Choi I, Romero MF, Khandoudi N, Bril A, Boron WF. Cloning and characterization of a human electrogenic  $Na^+-HCO_3^-$  cotransporter isoform (hhNBC). *Am J Physiol* 1999;276:C576–C584.
- [93] Pushkin A, Abuladze N, Newman D, Lee I, Xu G, Kurtz I. Cloning, characterization and chromosomal assignment of NBC4, a new member of the sodium bicarbonate cotransporter family. *Biochim Biophys Acta* 2000;1493:215–218.
- [94] Pushkin A, Abuladze N, Lee I, Newman D, Hwang J, Kurtz I. Cloning, tissue distribution, genomic organization, and functional characterization of NBC3, a new member of the sodium bicarbonate cotransporter family. *J Biol Chem* 1999;274:16569–16575.
- [95] Boron WF. Sodium-coupled bicarbonate transporters. *J Pancreas* 2001;2:176–181.
- [96] Geck P, Pietrzyk C, Burckhardt BC, Pfeiffer B, Heinz E. Electrically silent cotransport on  $Na^+$ ,  $K^+$  and  $Cl^-$  in Ehrlich cells. *Biochim Biophys Acta* 1980;600:432–447.
- [97] Frelin C, Chassande O, Lazdunski M. Biochemical characterization of the  $Na/K/Cl$  co-transport in chick cardiac cells. *Biochem Biophys Res Commun* 1986;134:326–331.
- [98] Liu S, Jacob R, Piwnica-Worms D, Lieberman M.  $(Na+K+2Cl)$  cotransport in cultured embryonic chick heart cells. *Am J Physiol* 1987;253:C721–C730.
- [99] Russell JM. Sodium-potassium-chloride cotransport. *Physiol Rev* 2000;80:211–276.
- [100] Gillen CM, Forbush III B. Functional interaction of the K-Cl cotransporter (KCC1) with the Na-K-Cl cotransporter in HEK-293 cells. *Am J Physiol* 1999;276:C328–C336.
- [101] Cleml HF, Feher JJ, Baumgarten CM. Modulation of rabbit ventricular cell volume and  $Na^+/K^+/2Cl^-$  cotransport by cGMP and atrial natriuretic factor. *J Gen Physiol* 1992;100:89–114.
- [102] Fry CH. Measurement and control of intracellular magnesium ion concentration in guinea pig and ferret ventricular myocardium. *Magnesium* 1986;5:306–316.
- [103] Buri A, Chen S, Fry CH et al. The regulation of intracellular  $Mg^{2+}$  in guinea-pig heart, studied with  $Mg^{2+}$ -selective microelectrodes and fluorochromes. *Exp Physiol* 1993;78:221–233.
- [104] Freudenrich CC, Murphy E, Liu S, Lieberman M. Magnesium homeostasis in cardiac cells. *Mol Cell Biochem* 1992;114:97–103.
- [105] Tashiro M, Konishi M. Sodium gradient-dependent transport of magnesium in rat ventricular myocytes. *Am J Physiol* 2000;279:C1955–C1962.
- [106] Rasgado-Flores H, Gonzalez-Serratos H. Plasmalemmal transport of magnesium in excitable cells. *Front Biosci* 2000;5:D866–D879.
- [107] Orchard CH, Kentish JC. Effects of changes of pH on the contractile function of cardiac muscle. *Am J Physiol* 1990;258:C967–C981.
- [108] Hulme JT, Orchard CH. Effect of acidosis on  $Ca^{2+}$  uptake and release by sarcoplasmic reticulum of intact rat ventricular myocytes. *Am J Physiol* 1998;275:H977–H987.
- [109] Choi HS, Trafford AW, Orchard CH, Eisner DA. The effect of acidosis on systolic  $Ca^{2+}$  and sarcoplasmic reticulum calcium content in isolated rat ventricular myocytes. *J Physiol* 2000;529:661–668.
- [110] Bers DM, Ellis D. Intracellular calcium and sodium activity in sheep heart Purkinje fibers: effect of changes of external sodium and intracellular pH. *Pflügers Arch* 1982;393:171–178.
- [111] Bielen FV, Bosteels S, Verdonck F. Consequences of  $CO_2$  acidosis for transmembrane  $Na^+$  transport and membrane current in rabbit cardiac Purkinje fibres. *J Physiol* 1990;427:325–345.
- [112] Harrison SM, Frampton JE, McCall E, Boyet MR, Orchard CH. Contraction and intracellular  $Na^+$ ,  $Ca^{2+}$  and  $H^+$  during acidosis in rat ventricular myocytes. *Am J Physiol* 1992;262:C348–C357.
- [113] Philipson KD, Bersohn MM, Nishimoto AY. Effects of pH on  $Na^+-Ca^{2+}$  exchange in canine cardiac sarcolemmal vesicles. *Circ Res* 1982;50:287–293.
- [114] Eigel BN, Hadley RW. Contribution of the  $Na^+$  channel and  $Na^+/H^+$  exchanger to the anoxic rise of  $[Na^+]$  in ventricular myocytes. *Am J Physiol* 1999;277:H1817–H1822.
- [115] Ju YK, Saint DA, Gage PW. Hypoxia increases persistent sodium current in rat ventricular myocytes. *J Physiol* 1996;497:337–347.
- [116] Undrovinas AI, Fleidervish IA, Makielski JC. Inward Na current at resting potentials in single cardiac myocytes induced by the ischemic metabolite lysophosphatidylcholine. *Circ Res* 1992;71:1231–1241.

- [117] Xiao XH, Allen DG. Role of  $\text{Na}^+/\text{H}^+$  exchanger during ischemia and preconditioning in the isolated rat heart. *Circ Res* 1999;85:723–730.
- [118] Crompton M, Capana M, Carafoli E. The sodium-induced efflux of calcium from heart mitochondria. A possible mechanism for regulation of mitochondrial calcium. *Eur J Biochem* 1976;69:453–462.
- [119] Crompton M. The regulation of mitochondrial Ca transport in heart. *Curr Top Memb Transp* 1985;25:231–276.
- [120] Jung DW, Baysal K, Brierley GP. The sodium-calcium antiport of mitochondria is not electroneutral. *J Biol Chem* 1995;270:672–678.
- [121] Fry CH, Powell T, Twist VW, Ward JPT. The effects of sodium, hydrogen and magnesium ions on mitochondrial calcium sequestration in adult rat ventricular myocytes. *Proc R Soc Lond* 1984;223:239–254.
- [122] Crompton M, Kunzi M, Carafoli E. The calcium-induced and sodium-induced effluxes of calcium from heart mitochondria. *Eur J Biochem* 1977;79:549–558.
- [123] Brierley GP, Baysal K, Jung DW. Cation transport systems in mitochondria:  $\text{Na}^+$  and  $\text{K}^+$  uniports and exchangers. *J Bioenerg Biomembr* 1994;26:519–526.
- [124] Rosen BP, Futai M. Sodium/proton antiporter of rat liver mitochondria. *FEBS Lett* 1980;117:39–43.
- [125] Kapus A, Lukacs GL, Cragoe Jr. EJ, Ligeti E, Fonyo A. Characterization of the mitochondrial  $\text{Na}^+/\text{H}^+$  exchange. The effect of amiloride analogues. *Biochim Biophys Acta* 1988;944:383–390.
- [126] Jung DW, Apel LM, Brierley GP. Transmembrane gradients of free  $\text{Na}^+$  in isolated heart mitochondria estimated using a fluorescent probe. *Am J Physiol* 1992;262:C1047–1055.
- [127] Arnon A, Hanlyn JM, Blaustein MP. Ouabain augments  $\text{Ca}^{2+}$  transients in arterial smooth muscle without raising cytosolic  $\text{Na}^+$ . *Am J Physiol* 2000;279:H679–H691.
- [128] Bielen FV, Glitsch HG, Verdonck F. Changes of the subsarcolemmal  $\text{Na}^+$  concentration in internally perfused cardiac cells. *Biochim Biophys Acta* 1991;1065:269–271.
- [129] Carmeliet E. A fuzzy subsarcolemmal space for intracellular  $\text{Na}^+$  in cardiac cells. *Cardiovasc Res* 1992;26:433–442.
- [130] Semb SO, Sejersted OM. Fuzzy space and control of  $\text{Na}^+/\text{K}^+$  pump rate in heart and skeletal muscle. *Acta Physiol Scand* 1996;156:213–224.
- [131] Su Z, Zou A, Nonaka A, Zubair I, Sanguinetti MC, Barry WH. Influence of prior  $\text{Na}^+$  pump activity on pump and  $\text{Na}^+/\text{Ca}^{2+}$  exchange currents in mouse ventricular myocytes. *Am J Physiol* 1998;275:H1808–H1817.
- [132] Terracciano CMN. Rapid inhibition of the  $\text{Na}^+/\text{K}^+$  pump affects  $\text{Na}^+/\text{Ca}^{2+}$  exchanger-mediated relaxation in rabbit ventricular myocytes. *J Physiol* 2001;533:165–173.
- [133] Wendt-Gallitelli MF, Voigt T, Isenberg G. Microheterogeneity of subsarcolemmal sodium gradients. Electron probe microanalysis in guinea-pig ventricular myocytes. *J Physiol* 1993;472:33–44.
- [134] Su Z, Sugishita K, Ritter M, Li F, Spitzer KW, Barry WH. The sodium pump modulates the influence of  $I_{\text{Na}}$  on  $[\text{Ca}^{2+}]_i$  transients in mouse ventricular myocytes. *Biophys J* 2001;80:1230–1237.
- [135] Lipp P, Niggli E. Sodium current-induced calcium signals in guinea-pig ventricular myocytes. *J Physiol* 1994;474:439–446.
- [136] Weber CR, Ginsburg KS, Bers DM. Cardiac  $\text{Na}$  current ( $I_{\text{Na}}$ ) does not elevate submembrane  $[\text{Na}]$  ( $[\text{Na}]_{\text{sm}}$ ) sensed by  $\text{Na}/\text{Ca}$  exchange (NCX). *Biophys J* 2002;82:565, (abstract).
- [137] Silverman BZ, Warley A, Miller JIA, James AF, Shattock MJ. Is there a transient rise in sub-sarcolemmal  $\text{Na}$  and activation of  $\text{Na}/\text{K}$ -pump current following activation of  $I_{\text{Na}}$  in ventricular myocardium. *Cardiovasc Res* 2003;57:1025–1034.
- [138] Goldhaber JJ, Lamp ST, Walter DO, Garfinkel A, Fukumoto GH, Weiss JN. Local regulation of the threshold for calcium sparks in rat ventricular myocytes: role of sodium–calcium exchange. *J Physiol* 1999;520:431–438.
- [139] Scriven DRL, Dan P, Moore EDW. Distribution of proteins implicated in excitation–contraction coupling in rat ventricular myocytes. *Biophys J* 2000;79:2682–2691.
- [140] Moore ED, Etter EF, Philipson KD et al. Coupling of the  $\text{Na}^+/\text{Ca}^{2+}$  exchanger,  $\text{Na}^+/\text{K}^+$  pump and sarcoplasmic reticulum in smooth muscle. *Nature* 1993;365:657–660.